OAK RIDGE NATIONAL LABORATORY
operated by
UNION CARBIDE CORPORATION
NUCLEAR DIVISION
for the
U.S. ATOMIC ENERGY COMMISSION

ORNL - TM - 2172

COPY NO. -

DATE - July 3, 1968

Neutron Physics Division

SEGO: A COMPUTER CODE FOR UNFOLDING EXPERIMENTAL PULSE-HEIGHT DISTRIBUTIONS

W. R. Burrus[+] and M. H. Young[‡]

A mathematical procedure is described for unfolding scintillation pulse-height spectra to obtain an estimate of the incident energy spectra. Two methods have been developed, both giving equivalent numerical answers. The first method, known as "Low Speed Sego," reduces the number of arithmetic operations for an N channel spectrum from the order of N^3 for conventional matrix inversion methods to the order of N^2 and simplifies the problem of constructing a model for the response of the spectrometer. The second method, known as "High Speed Sego," further reduces the number of arithmetic operations to the order of 10N instead of N^2. High Speed Sego makes use of the same ideas as Low Speed Sego and, in addition, transforms the response matrix of the spectrometer in such a way as to produce a large number of zero elements. This transformation is only applicable if the "Hyodo" response function can be represented by straight-line segments plus peaks (or by parabolic segments in a version under development known as "Double High Speed Sego). (NOTE: This report was prepared primarily as a description of Low-Speed Sego, since the high-speed modifications have been described elsewhere; however, an annotated version of the high-speed program is included here, along with the results obtained when the code was applied to the standard spectra measured by R. Heath with a 3 x 3 in. NaI(Tl) spectrometer.)

[+]Present address: Tennecomp, Inc., P. O. Box J, Oak Ridge, Tennessee.

[‡]ORAU Research Participant at ORNL during summers of 1965 and 1966.

NOTE: This Work Partially Supported by
NATIONAL AERONAUTICS AND SPACE ADMINISTRATION
Under Order R-104(1)

CONTENTS

Introduction†

The problem of correcting experimental distributions for instrumental smearing and aberations has long been solved for two cases. The first is when the smearing is symmetrical and the true distribution has an inherent or natural line width comparable to or broader than the instrumental smearing. The second is when the true distribution is known to be discrete with no continuous components. The first problem was essentially solved by Eddington[1] and the second by Gauss.[2]

In the present problem of gamma scintillation spectra, neither of the two above methods are applicable. The natural gamma-ray line width is negligible compared to the instrumental line width, and the spectrum consists of a continuous component and discrete components. Furthermore, the instrumental response is not symmetric but contains multiple peaks, tails, etc. Mathematically, the problem may be expressed as an integral equation. The desired solution must be obtained by statistical estimation, since the experimental pulse-height distributions are measured with a statistical uncertainty.

Traditionally, such problems in gamma-ray spectroscopy have been dealt with by *ad hoc* methods. One approach is to set up a large matrix equation and obtain the solution by a matrix inversion technique, but some procedure must be used to keep small experimental errors in the pulse-height distribution from being amplified in the result. Various techniques which have been used include: grouping the pulse-height data into rather large bins, suppressing negative components by means of special solution techniques, etc. Although these methods yield useful results, they have several difficulties:

---

†This report is primarily a description of Low Speed Sego, which was the code used to analyze the pulse height spectra representing the gamma rays given off by the Bulk Shielding Reactor II (see G. T. Chapman and W. R. Burrus, "Spectrum of Gamma Rays Emitted by a Stainless-Steel-Clad Pool-Type Reactor (BSR-II)," ORNL-TM 1284, 1968); a more detailed description of High Speed Sego can be found in an article by M. H. Young and W. R. Burrus ("A Digital Filter for Unfolding Pulse-Height Distributions") published in *Nucl. Instr. Methods* **62**, 82(1968).

a) A hundred or more pulse-height channels can be effectively used with modern scintillation spectrometers. Storing and inverting a matrix of this order demands the largest available computers so that frequently an ad hoc reduction of size is made resulting in loss of detail.

b) Usually the estimate of statistical uncertainty in the final results is nonexistent or not rigorous. If negative components are set to zero, for example, a valid confidence interval might still include nonzero values. This subtlety is usually ignored.

c) A major part of the overall problem is obtaining a catalog of calibration response functions. Although this is a straight-forward technical problem, much effort must be expended in suitably interpolating the calibration functions and in obtaining absolute calibrations.

The method used for analysis of our data alleviates many of the traditional problems. It has the following features:

a) The computation does not require that any matrix be stored. The amount of overall storage is of the order of 10 n locations (where n is the number of pulse-height channels) so that the method is practicable on small computers.

b) The algorithm requires only the solution to a triangular set of equations so that the number of computations is modest, being proportional to n^2.

c) A rigorous confidence interval for the resulting gamma spectrum is obtained.

d) The interpolation of the calibration spectra is handled automatically, and only a minimal of calibration information must be supplied to the program.

The "Sego" Unfolding Code

The Sego code transforms the pulse-height distribution (expressed in counts channel^{-1} sec^{-1}) into a gamma-photon distribution (expressed in photons MeV^{-1} sec^{-1} steradian^{-1}). The code corrects for the variable efficiency of the spectrometer and unfolds the Compton tails and escape peak from the pulse-height distribution. The method is superficially the same as that used by Zobel[3] and rediscovered many times since. In this description, we shall adopt a somewhat different point of view than that taken by Zobel.

The response of a scintillation spectrometer can be described by the integral equation

$$\int_0^\infty A_i(E')\varphi(E')dE' = b_i + e_i \quad i = 1, 2, \ldots, n \qquad (1)$$

where

b_i is the observed number of counts recorded in the ith channel of a multichannel analyzer which responds to pulses from V_i to V_{i+1} in height.

e_i is the random error in the counts in the ith channel due to statistical fluctuations. We assume that an estimate of e_i can be obtained from the data (subtraction of backgrounds can be taken properly into account in the usual manner).

$A_i(E')$ is the response function of the spectrometer; i.e., the probability that a photon source of unit intensity will produce a count in the ith channel.

$\varphi(E')dE'$ is the number of photons in the incident spectrum between an energy of E' and $E' + dE'$.

A two dimensional sketch of $A_i(E')$ is given in Fig. 1. Note that slices through this response surface parallel to the discrete channel number axis, $A_i(E')$ vs. i, are the conventional pulse-height distributions due to monoenergetic sources, but that slice through the response surface parallel to the energy axis, $A_i(E')$ vs. E' for fixed i, are "efficiency functions" which give the efficiency of a single channel for detection of a gamma photon.

Unfolding

As is well known, it is difficult to unfold the response of a spectrometer exactly without introducing spurious features into the desired result. Instead, what is often done (sometimes without saying so) is to leave some residual smearing in the final result so that the final gamma spectra calculated still contains some of the instrumental width. The major problem of the gamma scintillation spectrometer is not due to the instrumental smearing but is due to the

ORNL DWG 67-8522R

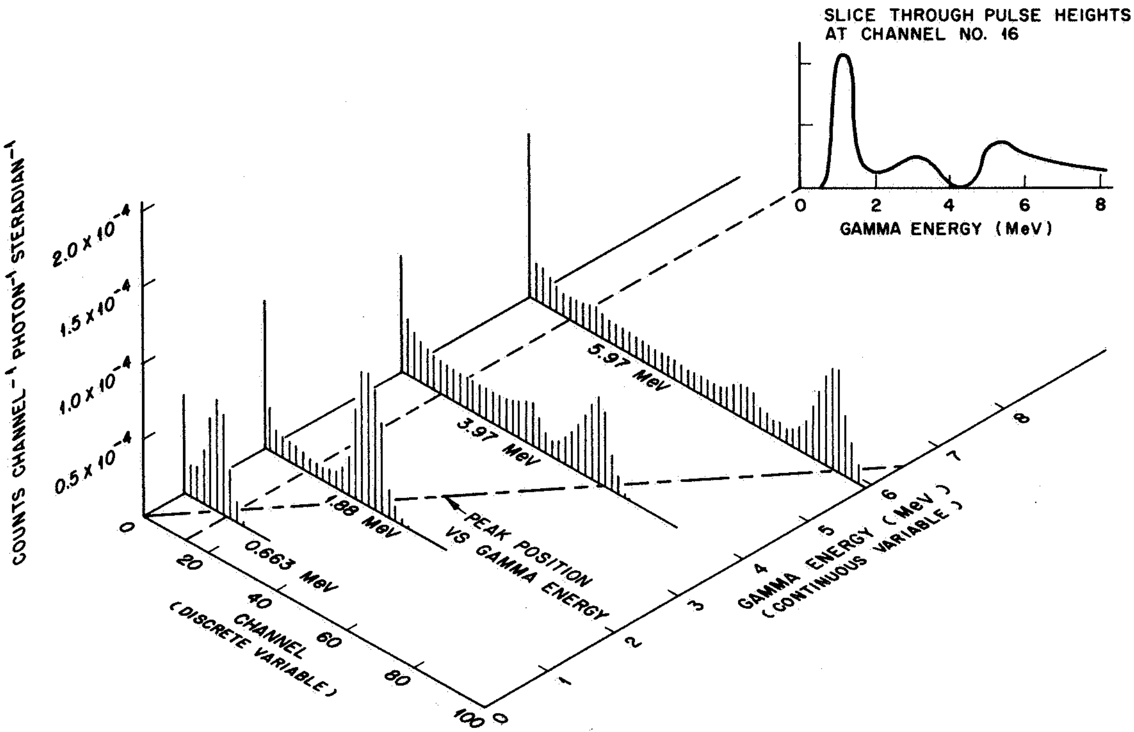

Fig. 1. Several Slices Through the Response Surface $A_i(E')$ for the 9 x 12 in. NaI(Tl) Spectrometer with Collimator.

fact that the monoenergetic response $A_i(E')$ has spurious peaks due to escape of pair production annihilation photons, etc. and a tail due to Compton scattered photons. Our approach is to admit from the beginning that we will accept the finite instrumental line width, and will try to remove the tails and spurious escape peak from the result. Let us denote the final estimated spectrum which we wish to compute by $\tilde{\varphi}(E)$. This estimated spectrum is related to the true spectrum $\varphi(E)$ by the relation

$$\tilde{\varphi}(E) = \int_0^\infty S(E, E')\varphi(E')dE' \quad . \tag{2}$$

Our problem now is that we are given a statistically uncertain b_i from the experiment, and we wish to compute $\tilde{\varphi}(E)$. We may in principle compute $\tilde{\varphi}(E)$ at many values of E arbitrarily selected. But because of the nonnegativity of $\varphi(E)$, Eq. (2) implies that $\tilde{\varphi}$ will be varying at least as slowly as $S(E, E')$. It is thus adequate to compute $\tilde{\varphi}(E)$ at energies E_k, $k = 1, 2, \ldots, n$ where the values of E_k are sufficiently close (say 2 to 3 per resolution width). We may think of the values of $\tilde{\varphi}(E_k)$ as the response of a conceptual pulse-height analyzer which has the response surface sketched in Fig. 2. This $W(E_k, E')$ response surface is similar to the $A_i(E')$ response surface sketched in Fig. 1 except that there is only one peak whose position is linearly related to gamma energy and whose efficiency is always constant.

The principal problem in obtaining the desired solution is finding a set of coefficients U_{ik}, $k = 1, 2, \ldots, n$ for each of the n response functions $A_i(E')$ such that

$$A_i(E') = \sum_{k=1}^{n} U_{ik}S(E_k, E') \quad . \tag{3}$$

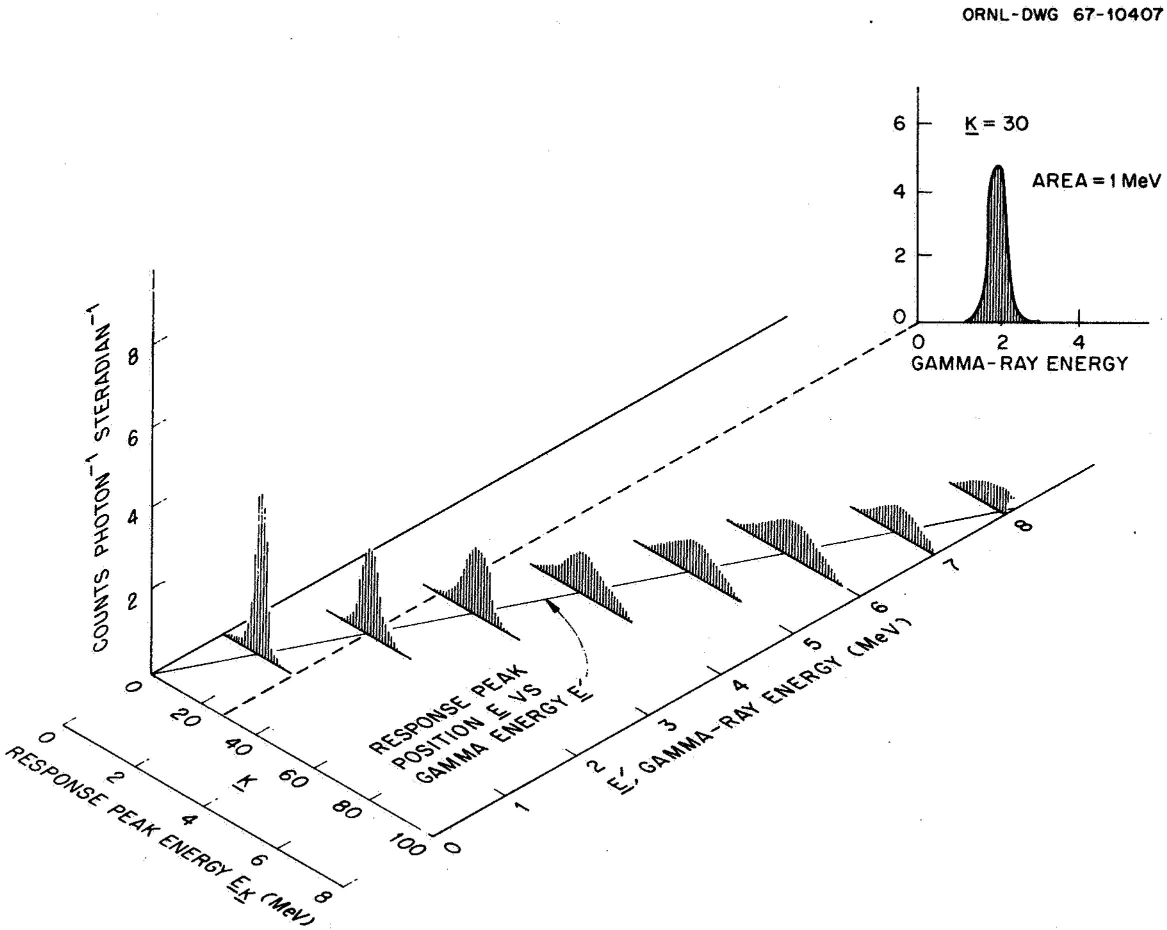

Fig. 2. Several Slices Through the Response Surface $W_k(E')$ for an "Ideal" Gamma-Ray Spectrometer.

We can achieve a rather large simplification if we accept the restriction that we will take the E_k, $k = 1, 2, \ldots, n$ to be the energies at which the main peaks of $A_i(E')$ vs. E' are centered.

In illustration, Fig. 3 shows a combination of $S(E_k, E')$ functions which adds up to a particular $A_i(E')$ function. By inspection of Fig. 3 we can see that it is not necessary to use any negative coefficients and that it is not necessary to use any $S(E_k, E')$ with E_k less than the center of the peak in the $A_i(E')$ function. If, for example, E_{70} is taken as the peak of the response function $A_{70}(E')$ as shown, the peak of $A_{70}(E')$ can be fit by a single $S(E_k, E')$ function of appropriate width. It is then necessary to add together a number of other $S(E_k, E')$ functions for higher values of E_k to match the upper "tail" and any other features the response function might display.

This fitting procedure is not necessarily unique, and it may well be possible to find several different sets of nonnegative coefficients U_{ik} which will give a satisfactory fit with the experimental error in measuring $A_i(E')$. Fortunately, the nonuniqueness of the U_{ik} does not result in a nonuniqueness of the result so long as Eq. (3) is satisfied.

In order to obtain a finite set of simultaneous algebraic equations for $\widetilde{\varphi}(E_k)$, substitute Eq. (3) into Eq. (1) to give:

$$\begin{aligned}
\int_0^\infty A_i(E')\varphi(E')dE &= b_i + e_i \qquad i = 1, 2, \ldots, n \\
&= \int_0^\infty \left[\sum_{k=1}^{n} U_{ik}\tilde{S}(E_k, E')\right]\varphi(E')dE' \qquad (4) \\
&= \sum_{k=1}^{n} U_{ik}\left[\int_0^\infty S(E_k, E')\varphi(E')dE'\right]
\end{aligned}$$

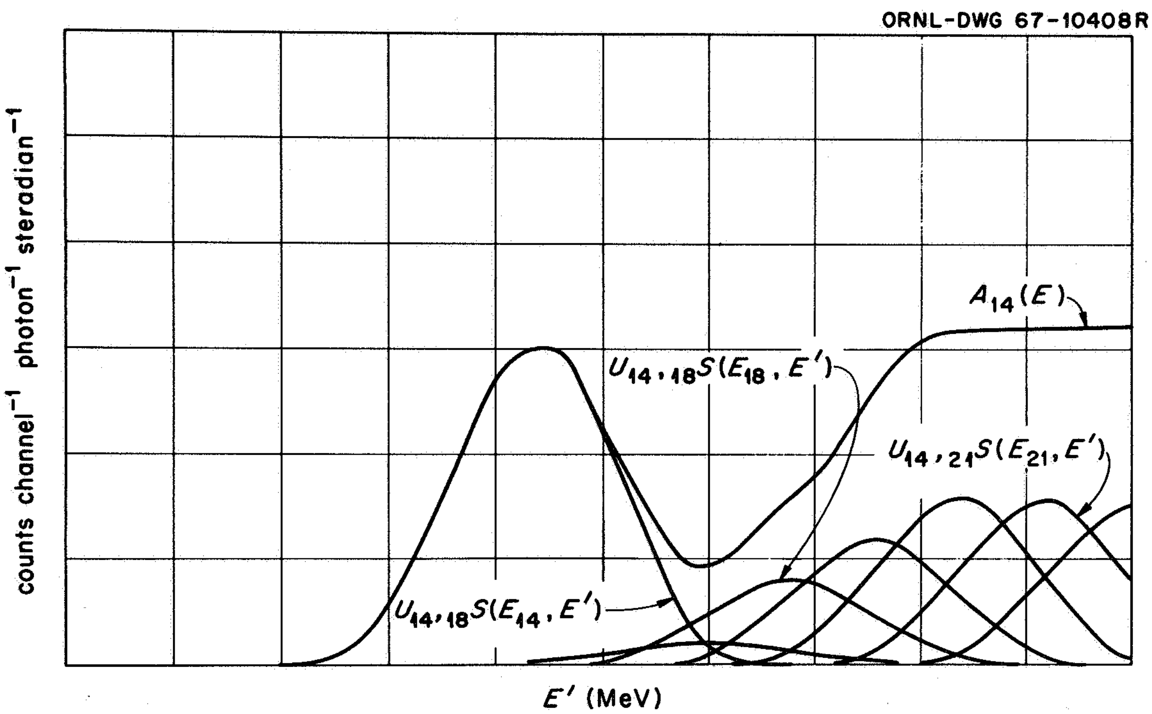

Fig. 3. An Illustration of the Combination of Several $S(E_k,E')$ Functions Which Add Up, with Weight Factors U_{ik}, to Give an $A_i(E)$ Response Function. For illustration, i = 14 is shown.

$$= \sum_{k=1}^{n} U_{ik}\tilde{\varphi}(E_k) \quad .$$

Note that we have interchanged the order of integration and summation and have made use of the definition of $\tilde{\varphi}(E)$ given by Eq. (2).

The estimated spectrum $\tilde{\varphi}(E)$ may be obtained directly from a solution of Eq. (4) using the measured b_i for an estimate of the right-hand side. Since it is not necessary to use any E_k less than the center of the peak of $A_i(E')$ in Eq. (4), the equations given by Eq. (4) have the triangular form

$$\begin{aligned}
U_{1,1}\tilde{\varphi}(E_1) + U_{1,2}\tilde{\varphi}(E_2) + \cdots + U_{1,n-1}\tilde{\varphi}(E_{n-1}) + U_{1,n}\tilde{\varphi}(E_n) &\approx b_1 \\
U_{2,2}\tilde{\varphi}(E_2) + \cdots \quad U_{2,n-1}\tilde{\varphi}(E_{n-1}) + U_{2,n}\tilde{\varphi}(E_n) &\approx b_2 \\
\cdots \qquad \cdots \qquad \cdots & \\
U_{n-1,n-1}\tilde{\varphi}(E_{n-1}) + U_{n-1,n}\tilde{\varphi}(E_n) &\approx b_{n-1} \\
U_{n,n}\tilde{\varphi}(E_n) &\approx b_n \quad .
\end{aligned} \tag{5}$$

By solving first for $\tilde{\varphi}(E_n)$ and then working backward toward $\tilde{\varphi}(E_1)$, we can minimize the amount of arithmetic required. This method of back substitution gives the solution simply as

$$
\begin{aligned}
\tilde{\varphi}(E_n) &\approx (1/U_{n,n})b_n \\
\tilde{\varphi}(E_{n-1}) &\approx (1/U_{n-1,n-1})[b_{n-1} - U_{n-1,n}\tilde{\varphi}(E_n)] \\
&\cdots \\
\tilde{\varphi}(E_j) &\approx (1/U_{jj})\Big[b_j - \sum_{k=j+1}^{n} U_{jk}\tilde{\varphi}(E_k)\Big] \\
&\cdots \\
\tilde{\varphi}(E_1) &= (1/U_{1,1})\Big[b_1 - \sum_{k=2}^{n} U_{ik}\tilde{\varphi}(E_k)\Big] \quad .
\end{aligned}
\tag{6}
$$

Statistical Error

Since we use the measured b_i as an estimate for the true $b_i + e_i$, the resultant estimate of $\tilde{\varphi}(E_j)$ will have some statistical uncertainty. In order to compute the standard error of the $\tilde{\varphi}(E_j)$, we could first express all the solutions of Eq. (5) in the inverse form:

$$
\begin{aligned}
\tilde{\varphi}(E_n) &= F_{n,n}b_n \\
\tilde{\varphi}(E_{n-1}) &= F_{n-1,n-1}b_{n-1} + F_{n-1,n}b_n \\
&\cdots \\
\tilde{\varphi}(E_1) &= F_{1,1}b_1 + \cdots + F_{1,n}b_n
\end{aligned}
$$

Then we could determine the estimated standard error in $\varphi(E_j)$ from the usual formula for the error in a sum

$$\sigma\left[\tilde{\varphi}(E_j)\right] = \sqrt{\sum_{i=1}^{n} F_{ji}^2 \sigma^2[b_i]} \quad . \tag{8}$$

But this calculation requires that the coefficients F_{ji} be available. Since we do not need the F_{ji} coefficients explicitly to obtain the solution $\tilde{\varphi}(E_j)$, it would be desirable to obtain the standard error of $\tilde{\varphi}(E_j)$ directly from the back solution scheme also, without the necessity of computing the inverse coefficients F_{ji}.

There does not seem to be an easy straightforward way of doing this. However a rather nice stochastic method is available based upon generating a set of random perturbations, d_i, by means of a numerical pseudo random number generator. This stochastic method allows the desired standard deviations to be obtained with many fewer arithmetic operations than would be required to evaluate the inverse coefficients F_{ji}. Furthermore, no extra computer storage is required. Suppose that we are given an experimentally measured pulse-height distribution b_i, $i = 1, 2, \ldots, n$, and the corresponding standard deviations s_i, $i = 1, 2, \ldots, n$. We can stochastically perturb the given b_i by adding to each term a randomly selected "normal deviate" chosen from the Gaussian distribution with mean 0 and standard deviation s_i. In this way we obtain a perturbed pulse-height distribution b_i', $i = 1, 2, \ldots, n$. Starting again with the experimental distribution b_i, $i = 1, 2, \ldots, n$, we can independently select another set of perturbations to obtain b_i'', $i = 1, 2, \ldots, n$, etc. as many times, r, as is desired.

Equation (5) is solved with each of the perturbed pulse-height distributions to give solutions $\tilde{\varphi}'(E_j)$, $j = 1, 2, \ldots, n$; $\tilde{\varphi}''(E_j)$, $j = 1, 2, \ldots, n$, etc. The standard deviation in $\tilde{\varphi}(E_j)$ can then be estimated from

$$\mathrm{std}\left[\tilde{\varphi}(E_j)\right] = \sqrt{\frac{1}{r - 1} \sum_{p=1}^{r} \left[\tilde{\varphi}^{(p)}(E_j) - \overline{\tilde{\varphi}(E_j)}\right]^2}$$

where $\overline{\tilde{\varphi}(E_j)}$ is the average of $\tilde{\varphi}'(E_j)$, $\tilde{\varphi}''(E_j)$, ..., $\tilde{\varphi}^{(r)}(E_j)$. As the number of perturbations r increases, the stochastic estimate of the desired standard deviation approaches that given by Eq. (8). The ratio between the result of Eq. (9) and Eq. (8) is given by $\sqrt{r/(r-1)}$ so that a choice of r anywhere from 3 to 10 is usually ample.

U Coefficient Method

Part of the raison d'être of the SEGO method is that a goodly portion of the work of unfolding is done in advance in the determination of the U_{ik} coefficients in Eq. (3). If one has many monoenergetic calibration sources, one may interpolate by suitable functions between the calibration sources and them determine the coefficients U_{ik} by a least squares fitting procedure. However, the problem of interpolating between available calibration energies is a formidable problem which we would like to simplify if possible. If the present case, we have made use of the physical characteristics of the response functions to reduce the amount of information needed to construct the U_{ik} coefficients.

The procedure we have used is to "parameterize" a simple piecewise continuous plus discrete approximation to the pulse-height distributions.

These parameters are listed in tabular form at convenient energies, and linear interpolation is used for intermediate values. Figure 4 shows the piecewise plus discrete representation of a typical pulse-height distribution which shows two escape peaks, a tail, and a backscatter peak. Since the position of the escape peaks and the "edge" of the tail can be accurately computed from simple formulas, sufficient parameters to characterized this distribution are

TOTAL EFFICIENCY
FIRST ESCAPE PEAK FRACTION
SECOND ESCAPE PEAK FRACTION
TAIL FRACTION
BACKSCATTER PEAK FRACTION
BACKSCATTER PEAK LOCATION
BACKSCATTER PEAK WIDTH.

The close resemblance between the U_{ik} coefficients and the pulse-height distributions is responsible for the convenience of the response surface representation. The primary difference seen in Fig. 4 is that the features of the parameterized distribution are more abrupt, with the total absorption and escape peaks being replaced by a single "spike" of about the same area. Similar the tail with a gradual "roll off" is replaced by a trapezoid with an abrupt fall. Finally the backscatter peak is replaced with a trapezoid of about the same width of the backscatter peak.

One may imagine that there is also a U_{ik} response surface which resembles the $A_i(E')$ response surface but which in general has more abrupt features. When the U_{ik} is smeared with the $S(E, E')$ function according to Eq. (3), the effect is to round off the abrupt edges so that the smeared U_{ik} surface will be identical to the $A_i(E')$ surface. It must be borne in mind that the smearing is not done along the channel number axis, but along the energy axis. Thus one can not apply the smoothing to a parameterized pulse-height distribution

ORNL-DWG 67-10409

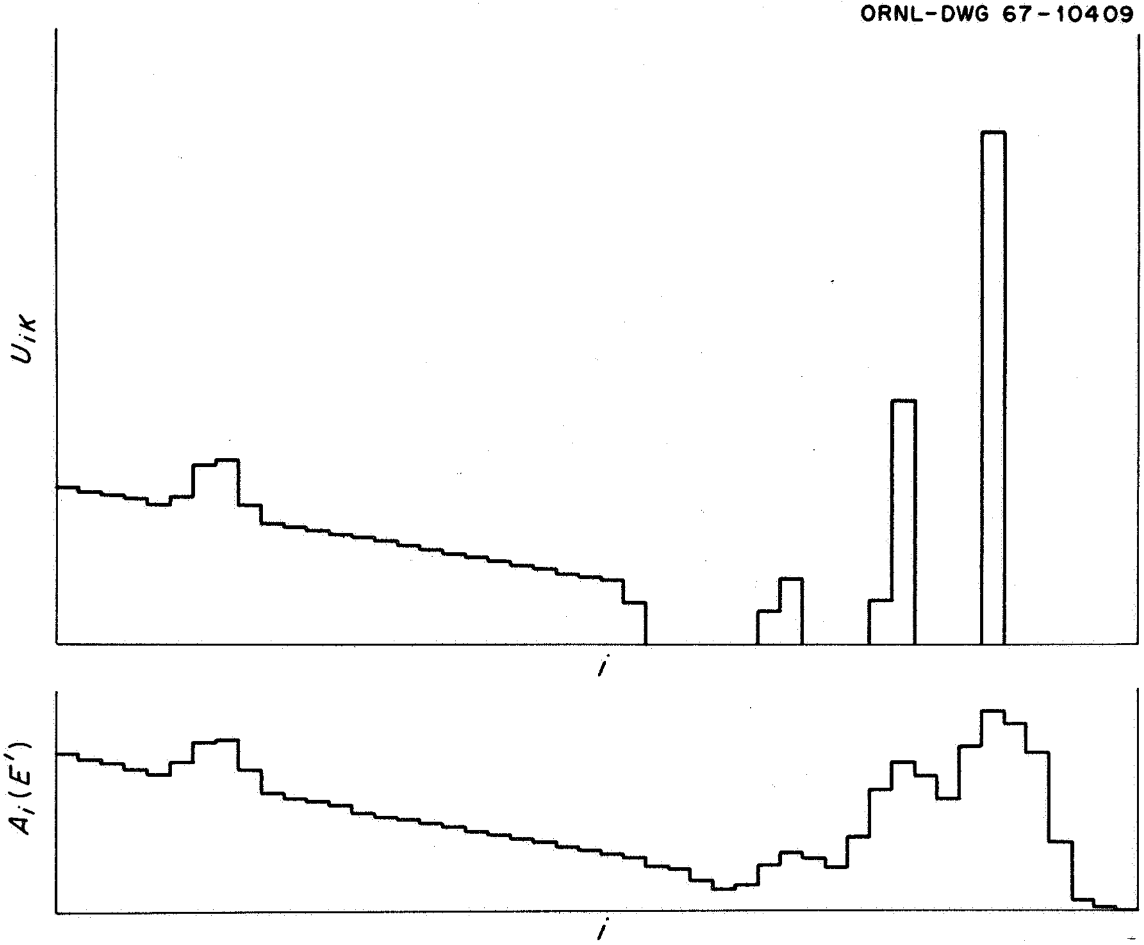

Fig. 4. Comparison of the Response Function $A_i(E')$, for a Particular Value of E', and the Discrete U_{ik} Representation for the Corresponding Energy E_k. The graphs show two escape peaks, a tail, and a backscatter peak in addition to the main total absorption peak at the right.

directly — the pulse-height distributions are slices of the response surface in the wrong direction. Instead one must parameterize a family of calibration pulse-height distributions, and then apply the $S(E, E')$ smearing by interpolating the parameterized distributions along the E' direction.

A little thought shows that the replacement of a peak by a "spike" is plausible if the location of the peak is proportional to energy, but not if the location of the peak is fixed (or almost fixed like the backscatter peak). In the case of a fixed peak, it is necessary to parameterize the width of the peak also.

In practice, a good method seems to be to guess the parameters from inspection of the calibration spectra, by approximately matching areas of the various parameterized features with the corresponding features in the monoenergetic calibration pulse-height distributions. Then the calibration spectra are unfolded by the method. Errors in the parameterization can then be corrected iteratively. The close correspondence of the parameters to physical features of the pulse-height distribution makes it easy to "tune out" an objectionable bump in the final result by varying the value of the paremeter. Of course the total efficiency of the parameterized functions and the "natural" functions must be kept the same in order to insure that the absolute magnitude of the result is correct.

If one wished to obtain the parameters from first principles without experimental "adjustment", one could construct a model of the entire "natural" response function, and then use a least squares fitting procedure to obtain the best match between the natural response function and the smeared parameterized response function. But this would be failing completely to make use of the spirit and advance of the method which was formulated precisely to make such tedious fitting unnecessary.

The final parameters adopted for a 9 by 12 in. collimated NaI(Tl) crystal are given in Table 1. These parameters were based on matching calibration spectra from ^{24}Na, ^{88}Y, ^{16}N, and ^{137}Cs sources placed outside the collimator and along its axis. The absolute efficiencies are based on geometry and total gamma-ray cross sections of NaI, modified by a collimator correction. Backscatter and second escape peak fractions were negligible and thus are not included.

Table 1. Parameters for 9 x 12 in.
Collimated NaI(Tl) Crystal

Energy (MeV)	Peak/Total Ratio	Tail Edge (MeV)	First Escape Fraction	ε(E), Efficiency (counts-cm^2-ster/photon)
				x 10^{-6}
0	1.00	0	0	3.27
0.25	0.927	0.124	0	3.45
0.50	0.889	0.331	0	3.77
0.75	0.864	0.559	0	4.07
1.00	0.845	0.796	0	4.37
1.25	0.830	1.04	0.0008	4.51
1.50	0.820	1.28	0.0024	4.80
1.75	0.814	1.53	0.0046	4.94
2.00	0.809	1.77	0.0082	5.07
2.25	0.808	2.02	0.0116	5.14
2.50	0.808	2.27	0.0151	5.20
2.75	0.806	2.52	0.0184	5.23
3.00	0.804	2.76	0.0213	5.27
3.25	0.801	3.01	0.0248	5.28
3.50	0.800	3.26	0.0279	5.29
3.75	0.800	3.51	0.0306	5.29
4.00	0.800	3.76	0.0334	5.28
4.25	0.800	4.01	0.0360	5.27
4.50	0.802	4.26	0.0385	5.26
4.75	0.804	4.51	0.0408	5.24
5.00	0.805	4.76	0.0435	5.24
5.25	0.808	5.01	0.0452	5.22
5.50	0.811	5.26	0.0475	5.19
5.75	0.814	5.51	0.0496	5.17
6.00	0.817	5.76	0.0515	5.15
6.25	0.821	6.00	0.0535	5.14
6.50	0.824	6.25	0.0556	5.12
6.75	0.827	6.50	0.0576	5.11
7.00	0.830	6.75	0.0592	5.09
7.25	0.834	7.00	0.0611	5.07
7.50	0.836	7.25	0.0628	5.06
7.75	0.839	7.50	0.0644	5.04
8.00	0.842	7.75	0.0658	5.02
8.25	0.844	8.00	0.0678	5.01
8.50	0.846	8.25	0.0692	5.00
8.75	0.848	8.50	0.0708	4.99
9.00	0.850	8.75	0.0722	4.97
9.25	0.852	9.00	0.0737	4.96
9.50	0.854	9.25	0.0750	4.94
9.75	0.855	9.50	0.0765	4.93
10.00	0.856	9.75	0.0780	4.92
10.25	0.857	10.0	0.0792	4.90
10.50	0.858	10.3	0.0805	4.89
10.75	0.860	10.5	0.0819	4.88
11.00	0.861	10.6	0.0831	4.87
11.25	0.862	11.0	0.0844	4.85
11.50	0.864	11.3	0.0858	4.84
11.75	0.865	11.5	0.0870	4.83
12.00	0.866	11.7	0.0881	4.82

REFERENCES

1. A. S. Eddington, Monthly Notices Roy. Astron. Soc., Vol. 73, pp. 359-360 (1913) (also see extensive discussion in following issues).

2. C. F. Gauss, Methodé des Moindres Carrés (Translated by J. Bertrand, Paris) (1855). See also R. L. Plackett, "A Historical Note on the Method of Least Squares," Biometrika, Vol. 36, pp. 548-560 (1949).

3. W. Zobel, T. A. Love, G. M. Estabrook, and R. W. Peelle, "Characteristics of Fission-Product Gamma Rays Emitted from 1 to 1800 sec After Thermal Fission of ^{235}U," Neutron Physics Division Annual Progress Report, ORNL-2609, pp. 50-51 (1958).

Appendix I. Main FORTRAN Subroutines for Low Speed SEGO

The two main FORTRAN routines are attached as an APPENDIX. The main routine which performs the back substitution is called SEGO. The A(I,J) routine calculates the values of the response as they are needed by SEGO. The calling program must have already prepared an appropriate list of PTOT (peak to total ratio), EDGE (Compton edge location in channels), SLOPE (slope of the Compton tail), and TAIL (the average height of the Compton tail). Escape peaks are not included in this version but their addition is trivial.

```
      SUBROUTINE SEGO(C,SC,G,N)
C
C     SUBROUTINE SEGO IS  A SIMPLE BACK SUBSTITUTION ROUTINE....
C     BUT 9 ADDITIONAL SOLUTIONS ARE COMPUTED BY CALCULATING PERTURBED
C     DATA....  BERFN IS AN INVERSE ERROR FUNCTION ROUTINE FOR
C     GENERATING NORMAL RANDOM DEVIATES.......
C     A(I,J) IS A SUBROUTINE WHICH RETURNS THE RESPONSE MATRIX ELEMENTS
C
      DIMENSION C(402),SC(402),G(402,10)
C     BACK SUBSTITUTE FOR 10 PERTURBED SOLUTIONS
      DO   29   II = 1,N
                I = N-II+1
      G(I,1) = C(I)
           DO   16   L = 2,10
16         G(I,L) = C(I) + SC(I) * BERFN(RANF(0)-0.5)
           IF   (I-N)   18,22,22
18         III = I+1
                DO   20   K = III,N
                AIK = A(I,K)
                DO   20   L = 1,10
20              G(I,L) = G(I,L) - AIK*G(K,L)
22              AII = 1.0/A(I,I)
                DO   29   L = 1,10
29              G(I,L) = G(I,L) * AII
      RETURN
      END
```

```
      FUNCTION A(I,J)
C
C          THIS SUBROUTINE GENERATES THE HY500 RESPONSE MATRIX. THE
C     EFFICIENCY CORRECTION IS DEFERRED SO THAT THE RESULTING SPECTRA
C     MAY BE COMPARED DIRECTLY WITH THE  RAW COUNT DATA, C(I).....
C     THE RESULTING SPECTRA SHOULD LATER BE DIVIDED BY THE EFFICIENCY,
C     THAT IS EFF(J).....
C
      COMMON  PTOT(402),EDGE(402),SLOPE(402),EFF(402),TAIL(402)
C
   30 IF(I-J)34,32,33
   32 A=PTOT(J)
      GO TO 35
   33 WRITE (51,933)
  933 FORMAT(29H0YOU CANT GET THERE FROM HERE)
      GO TO 88
   34 A=0.0
   35 FI=I
      IF(EDGE(J)+1.0-FI)88,88,38
   38 DIF=EDGE(J)-FI
      TILT=1.0+SLOPE(J)*((2.0*FI-EDGE(J))/EDGE(J))
      IF(DIF)40,40,41
   40 A=TILT*((1.0+DIF)*TAIL(J)/EDGE(J))+A
      GO TO 88
   41 A=TILT*(TAIL(J)/EDGE(J))+A
   88 RETURN
      END
```

Appendix II. High Speed SEGO

The following pages give an annotated version of the program described in an article accepted for publication in Nuclear Instruments and Methods (see M. H. Young and W. R. Burrus, "A Digital Filter for Unfolding Pulse-Height Distributions").

SEGO - EFN SOURCE STATEMENT - IFN(S) -

```
C
C     ##########################################################
C     # SEGO UNFOLDING FILTER.  CALLS THE SUBROUTINE REBIN     #
C     # IF LINEARITY CORRECTION IS DESIRED.                    #
C     ##########################################################
C
C
      PROGRAM SEGO
      DIMENSION B(400),XRUN(4),PLOT(61),EF(21),ES(21),PT(21),
     1   EC(21),BK(21),X(400,4),VU(21),VL(21),VH(21),ID(32)
      COMMON B
C
C     ********************************************************
C1    * READ IN THE PLOTTING SYMBOLS, THE RESPONSE PARAMETERS*
C     * (TOTAL EFFICIENCY, PEAK TO TOTAL RATIO, FIRST ESCAPE *
C     * PEAK TO TOTAL FRACTION, SECOND ESCAPE PEAK TO TOTAL  *
C     * FRACTION, BACK SCATTERING PEAK TO TOTAL FRACTION,    *
C     * VALLEY-FILL FUNCTION UPPER EDGE IN MEV, VALLEY-FILL  *
C     * FUNCTION LENGTH IN MEV, AND VALLEY-FILL FUNCTION TO  *
C     * TOTAL FRACTION), NO. OF CHANNELS, CHANNEL WIDTH (MEV/*
C     * CH), ZERO ENERGY CHANNEL, CHANNEL-COMBINATION FACTOR *
C     * (USE EVERY CHANNEL IF CHFT#1.,USE BINS OF TWO GROUPED*
C     * CHANNELS IF CHFT#2.), REBIN BYPASS COMMAND, IDENTIFI-*
C     * CATION OF THE SPECTRUM, AND THE SPECTRUM (COUNTS/CH.)*
C     ********************************************************
C
    1 READ(5,100)PLOT,SYM1,SYM2
  100 FORMAT(61A1,2A1)
    2 READ(5,101)(EF(M),PT(M),ES(M),EC(M),BK(M),VU(M),VL(M)
     1   ,VH(M),M#1,21)
  101 FORMAT(7XE9.2,F7.4,7X,6F7.4)
      WRITE (6,109)
  109 FORMAT(1H1)
      DO 999 JJ#2,21
      VL(JJ)#.333*VL(JJ)
  999 VH(JJ)#1.5*VH(JJ)
      WRITE(6,99)(EF(M),PT(M),ES(M),EC(M),BK(M),VH(M),VU(M)
     1   ,VL(M),M#1,21)
   99 FORMAT(7XE9.2,7F10.4)
    3 READ (5,107) N,G,ZO,CHFT,NRB,ID
  107 FORMAT(I3,3F10.5,I7,32A1)
      IF (N) 45,45,4
    4 READ (5,103) (B(M),M#1,N)
      WRITE (6,109)
      WRITE(6,103) (B(M),M#1,N)
  103 FORMAT(12X,10F6.0)
      ESP#.511/G
      BW#8./CHFT
      KH#BW/2.
      IF(NRB)6,6,5
C
C     *********************************************************
C2    * NBR#1 TO REBIN, NBR#0 FOR LINEAR GAIN (BYPASS REBIN).*
C     *********************************************************
C
    5 CALL REBIN(N,G,ZO,CHFT)
```

```
      WRITE(6,103) (B(M),M#1,N)
C
C    ***********************************************************
C3   * PLOTTING SCALE FACTOR DETERMINATION.                    *
C    ***********************************************************
C
    6 BIGST # 0.
      DO 8 I#1,N
      FJ#I
      ENERGY#(FJ-ZO)*G
      IE#2.*ENERGY
      Z#2.*ENERGY-FLOAT(IE)
      EFF#(1.-Z)*EF(IE+1)+Z*EF(IE+2)
      DIAG#(1.-Z)*PT(IE+1)+Z*PT(IE+2)
      TERM # B(I)/(EFF*DIAG)
      IF(BIGST - TERM) 7,7,8
    7 BIGST # TERM
    8 CONTINUE
      S#50./BIGST
      WRITE(6,102) N,G,ZO,S,CHFT,NRB
  102 FORMAT(1X,I3,2F10.5,E10.3,F10.2,I7)
C
C    ***********************************************************
C4   * PERTURBING THE SPECTRUM 4 TIMES BY A RANDOM NUMBER      *
C    * SCHEME.                                                 *
C    ***********************************************************
C
      NRAN#78125
      DO 10 I#1,N
      X(I,1)#B(I)
      SQ#SQRT(B(I)+0.5)
      DO 10 L#2,4
      NRAN#MOD(NRAN*78125,32768)
      RAN#3.0517578E-5*FLOAT(NRAN)-0.5
      T#SQRT(-(ALOG((0.5-ABS(RAN))**2)))
      BERF#T-(2.30753+.27061*T)/(1.+T*(.99229+.04481*T))
      BERF#SIGN(BERF,RAN)
   10 X(I,L)#B(I)+SQ*BERF
C
C    ***********************************************************
C4.5* OBTAIN DIFFERENTIAL SPECTRUM.                            *
C    ***********************************************************
C
      DO 15 L#1,4
      X(N+1,L)#0.
      DO 15 I#1,N
   15 X(I,L)#X(I,L)-X(I+1,L)
C
C    ***********************************************************
C5   * INITIATING OF THE MAIN LOOP.                            *
C    ***********************************************************
C
      XRUN(1)#0.
      XRUN(2)#0.
      XRUN(3)#0.
      XRUN(4)#0.
```

```
      J#N+1
      WRITE (6,109)
      WRITE (6,104) ID,S
  104 FORMAT(5X29HRUNSUM   RSPLOT  ERACC ENERGY,3X,32A1,3X,
     1       9HP-SCALE #,E11.4)
C
C    **********************************************************
C6   * THE MAIN LOOP.                                         *
C    **********************************************************
C
      DO 40 JJ#1,N
      J#J-1
      JJJ#J-1
      AUP#-1.E30
      ALO#1.E30
      FJ#J
      ENERGY#(FJ-Z0)*G
      IE#2.0*ENERGY
      Z#2.0*ENERGY-FLOAT(IE)
      Y#1.-Z
      IE1#IE+1
      IE2#IE+2
C
C    **********************************************************
C7   * CALCULATE THE JTH SHAPE PARAMETERS BY INTERPOLATION.   *
C    **********************************************************
C
      EFF#Y*EF(IE1)+Z*EF(IE2)
      ESC1#Y*ES(IE1)+Z*ES(IE2)
      ESC2#Y*EC(IE1)+Z*EC(IE2)
      BKSP#Y*BK(IE1)+Z*BK(IE2)
      DIAG#Y*PT(IE1)+Z*PT(IE2)
      VFUP#Y*VU(IE1)+Z*VU(IE2)
      VFWE#Y*VL(IE1)+Z*VL(IE2)
      VFAF#Y*VH(IE1)+Z*VH(IE2)
C
C    **********************************************************
C8   * CALCULATE THE VALLEY FILLED FUNC. POSITION AND HEIGHT*
C    **********************************************************
C
      FUP#VFUP/G+Z0+0.5
      VFW#VFWE/G
      FLO#FUP-VFW
      KU#FUP
      KL#FLO
      FU#FUP-FLOAT(KU)
      FL#FLO-FLOAT(KL)
      VFHT#VFAF/VFW
C
C    **********************************************************
C9   * CALCULATE THE COMPTON EDGE POSITION AND TAIL HEIGHT.   *
C    **********************************************************
C
      EDGE#ENERGY/(1.+.2555/ENERGY)
      EGG#EDGE/G
      TAIL#(1.-DIAG-ESC1-ESC2-BKSP-VFAF)/EGG
```

```
        SEGD          -  EFN   SOURCE STATEMENT  -  IFN(S)  -

       FKEDG#EGG+Z0+0.5
       KEDG#FKEDG
       FTAIL#FKEDG-FLOAT(KEDG)
C
C    ******************************************************
C10 * CALCULATE THE POSITIONS OF THE BACK SCATTERING AND   *
C   * THE FIRST AND SECOND ESCAPE PEAKS.                  *
C    ******************************************************
C
       KB#FJ-EGG+0.5
       K1#KB+KH
       K2#KB-KH
       KA#FJ-ESP+0.5
       KC#FJ-2.*ESP+0.5
C
C    ******************************************************
C11 * THE SUBTRACTION LOOP FOR THE 4 PERTURBED SPECTRA.    *
C    ******************************************************
C
       DO 35 L#1,4
       ANS#X(J,L)/DIAG
       X(J,L)#ANS
C
C    ******************************************************
C12 * CALCULATE THE RUNNING SUM OF THE UNSCRAMBLED SPECTRUM*
C   * AND THE UPPER AND LOWER RUNNING LIMITS.              *
C    ******************************************************
C
       XRUN(L)#XRUN(L)+ANS/EFF
       AUP#AMAX1(AUP,XRUN(L))
       ALO#AMIN1(ALO,XRUN(L))
C
C    ******************************************************
C13 * THE SUBTRACTION SCHEME OF THE DIFFERENTIAL SPECTRUM. *
C    ******************************************************
C      CALCULATE THE (J-1)TH X.
       IF(JJJ)35,35,16
    16 X(JJJ,L)#X(JJJ,L)+ANS*DIAG
C      REMOVE THE COMPTON TAIL.
       IF(KEDG-1)25,25,17
    17 X(KEDG-1,L)#X(KEDG-1,L)-ANS*TAIL*(1.-FTAIL)
       X(KEDG,L)#X(KEDG,L)-ANS*TAIL*FTAIL
C      REMOVE THE FIRST ESCAPE PEAK.
       IF(KA-1)23,23,20
    20 X(KA-1,L)#X(KA-1,L)+ANS*ESC1
       X(KA,L)#X(KA,L)-ANS*ESC1
C      REMOVE THE SECOND ESCAPE PEAK.
       IF(KC-1)23,23,22
    22 X(KC-1,L)#X(KC-1,L)+ANS*ESC2
       X(KC,L)#X(KC,L)-ANS*ESC2
C      REMOVE THE BACK SCATTERING PEAK.
    23 IF(KH)25,25,24
    24 X(K1,L)#X(K1,L)-ANS*BKSP/BW
       IF(K2)25,25,18
    18 X(K2,L)#X(K2,L)+ANS*BKSP/BW
C      REMOVE THE VALLEY FILLED FUNCTION.
```

```
         SEGO        - EFN   SOURCE STATEMENT  -  IFN(S)  -

   25 IF(KU-1)35,35,26
   26 X(KU-1,L)#X(KU-1,L)-ANS*VFHT*(1.-FU)
      X(KU,L)#X(KU,L)-ANS*VFHT*FU
   27 IF(KL-1)35,35,28
   28 X(KL-1,L)#X(KL-1,L)+ANS*VFHT*FL
      X(KL,L)#X(KL,L)+ANS*VFHT*(1.-FL)
   35 CONTINUE
C
C   ***********************************************************
C14 * EVALUATE THE ERROR FROM THE UPPER AND THE LOWER        *
C   * LIMITS OF THE PERTURBED SPECTRA.                        *
C   ***********************************************************
C
   36 XRS#XRUN(1)*S
      ERACC#.6*(AUP-ALO)*S
      KX#10.5+X(J,1)*S/EFF
      KX#MINO(MAXO(KX,1),61)
C
C   ***********************************************************
C15 * PLOT THE UNSCRAMBLED SPECTRUM.                          *
C   ***********************************************************
C
      SAVE*PLOT(KX)
      PLOT(KX)#SYM1
      WRITE(6,105)XRUN(1),XRS,ERACC,ENERGY,(PLOT(L),L#1,KX)
   40 PLOT(KX)#SAVE
  105 FORMAT(1XE12.5,F7.2,F7.3,F7.2,61A1)
      GO TO 3
   45 STOP
      END
```

```
C     ############################################################
C     # SUBROUTINE TO MAKE LINEARITY CORRECTION.                 #
C     # THIS VERSION USES R. HEATH 5TH ORDER POLYNOMIAL FOR      #
C     # THE 3 IN. X 3 IN. NA-I(TL) DETECTOR.                     #
C     ############################################################
C
      SUBROUTINE REBIN(N,G,Z0,CHFT)
      DIMENSION SUM(200),B(200)
      COMMON B
      DO 5 K#1,200
    5 SUM(K)#0.
C
C     ************************************************************
C     * TO FORM A RUNNING SUM.                                   *
C     ************************************************************
C
      DO 10 J#1,N
      I#N-J+1
   10 SUM(I+1)#SUM(I+2)+B(I)
      SUM(1)#SUM(2)+B(1)
      DO 20 J#1,N
C
C     ************************************************************
C     * CALCULATE THE ENERGIES AT THE UPPER AND LOWER EDGES      *
C     * OF A CHANNEL AND CONVERT THEM TO CHANNELS BY THE         *
C     * NON-LINEAR ENERGY TO CHANNEL RELATIONSHIP.               *
C     ************************************************************
C
      EUP#G*(FLOAT(J)-Z0+.5)
      CUP#.40715+103.08984*EUP-6.60938*EUP**2+2.55859*EUP**3
     1     -0.52246*EUP**4+0.041382*EUP**5
      ELO#EUP-G
      CLO#.40715+103.08984*ELO-6.60938*ELO**2+2.55859*ELO**3
     1     -0.52246*ELO**4+0.041382*ELO**5
C     CORRECTION FOR BINED CHANNELS.
      CUP#CUP/CHFT
      CLO#CLO/CHFT
C
C     ************************************************************
C     * EVALUATE THE CORRESPONDING RUN SUMS AT THE UPPER AND     *
C     * LOWER EDGES OF THE REVISED CHANNELS AND OBTAIN THE       *
C     * DIFFERENCES TO GIVE THE REBINED COUNTS.                  *
C     ************************************************************
C
      NUP#CUP
      NLO#CLO
      FUP#CUP-FLOAT(NUP)
      FLO#CLO-FLOAT(NLO)
      VALUP#(1.-FUP)*SUM(NUP+1)+FUP*SUM(NUP+2)
      VALLO#(1.-FLO)*SUM(NLO+1)+FLO*SUM(NLO+2)
   20 B(J)#VALLO-VALUP
      WRITE(6,110)
  110 FORMAT(16H REBIN COMPLETED)
      RETURN
      END
```

App. III. Results from High Speed SEGO

Graphs of pulse-height distributions and unfolded spectra produced by High Speed Sego follow. These results were obtained by applying the code to the data of R. Heath obtained with a 3 x 3 in. NaI(Tl) spectrometer.

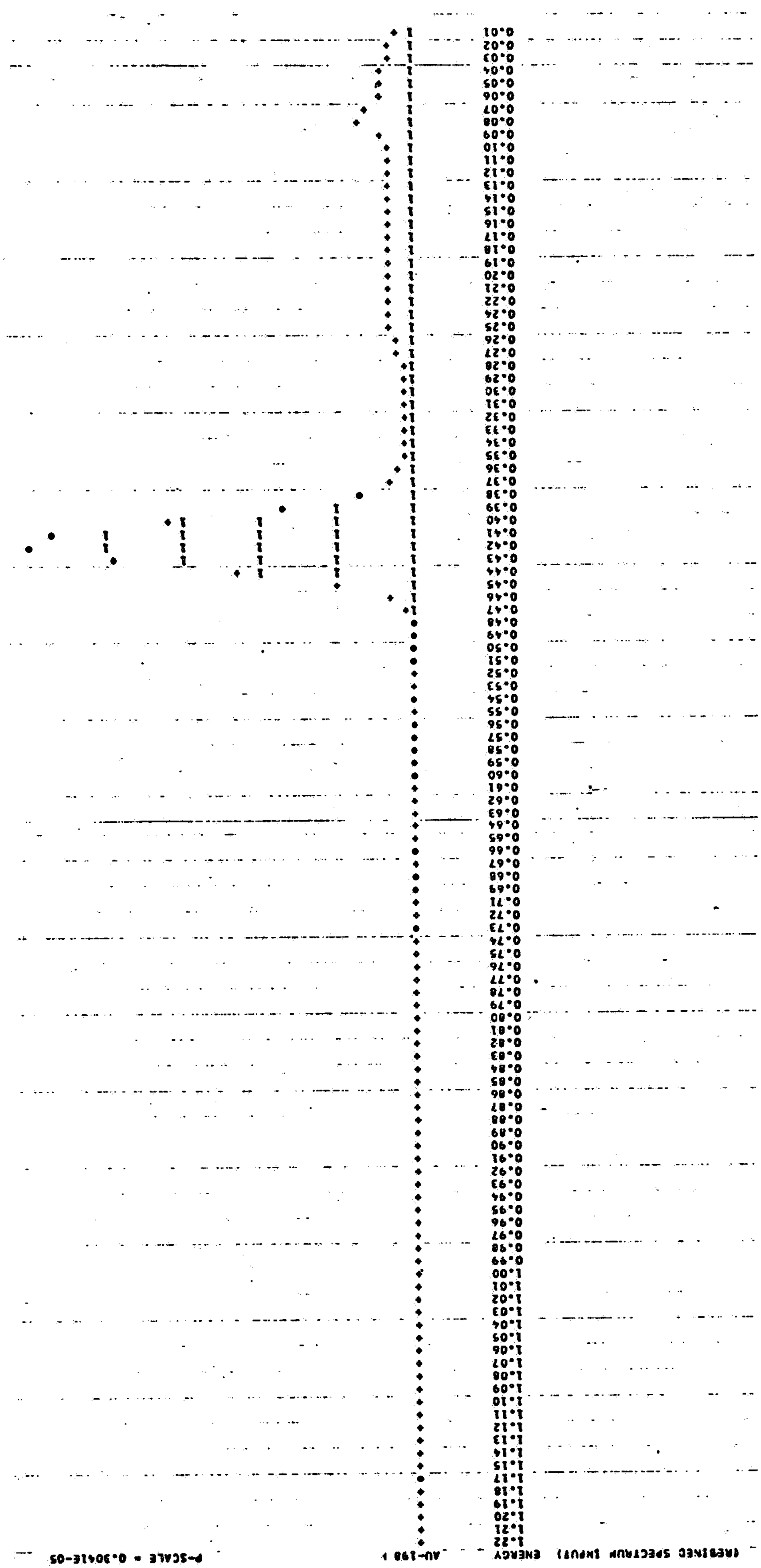

Fig. III-1. Corrected Pulse-Height Distribution for ^{178}Au.

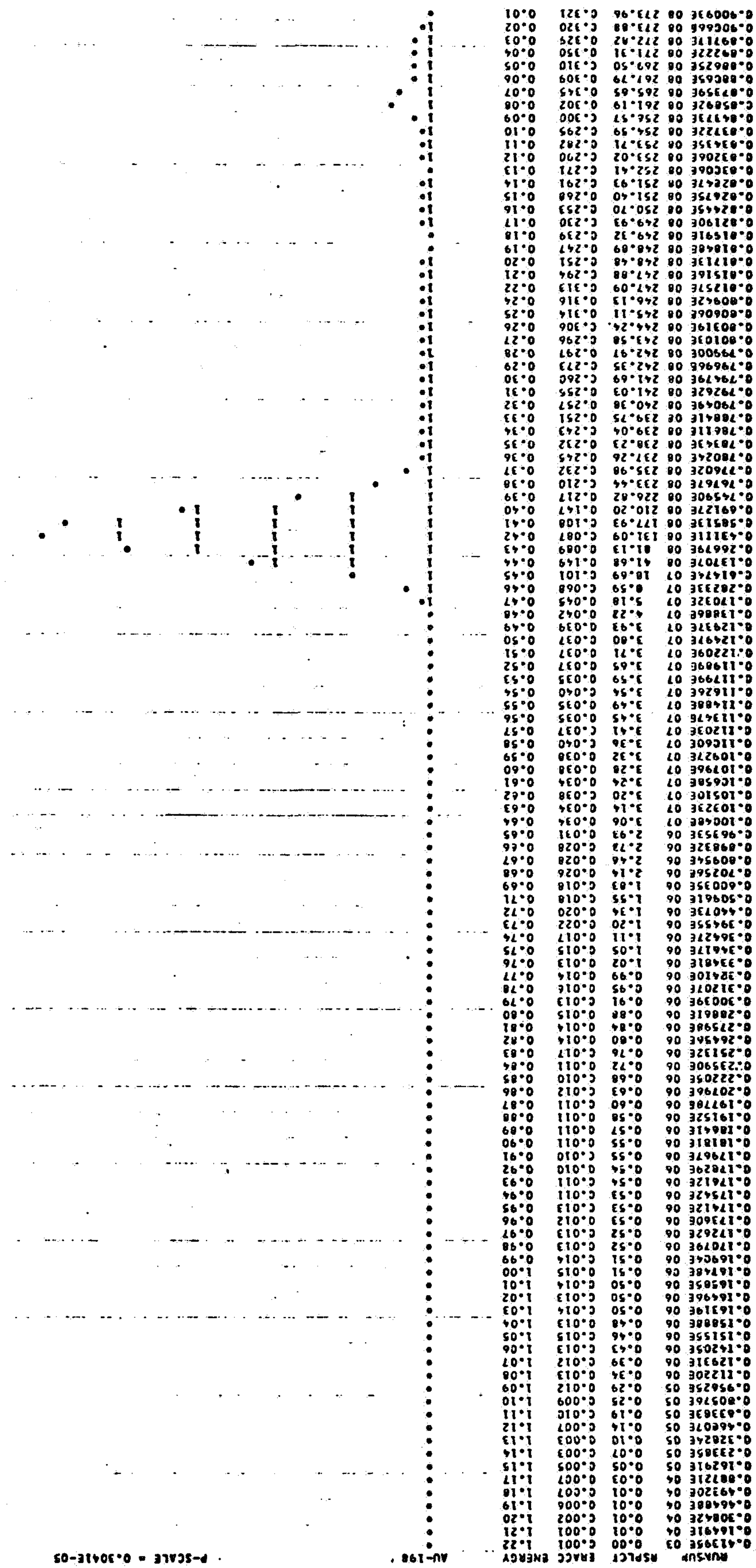

Fig. III-2. Unfolded Gamma Spectrum for ^{178}Au.

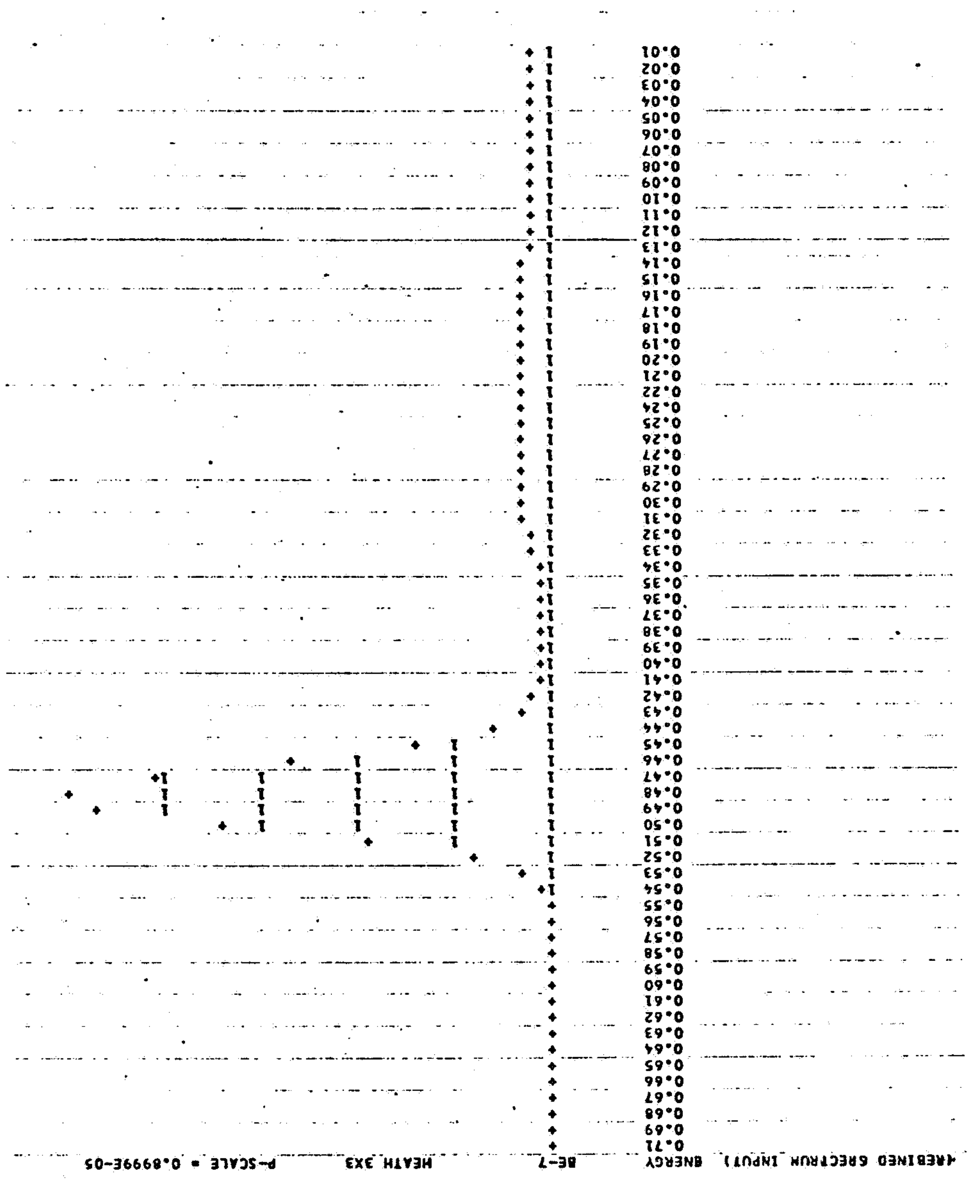

Fig. III-3. Corrected Pulse-Height Distribution for ^{7}Be.

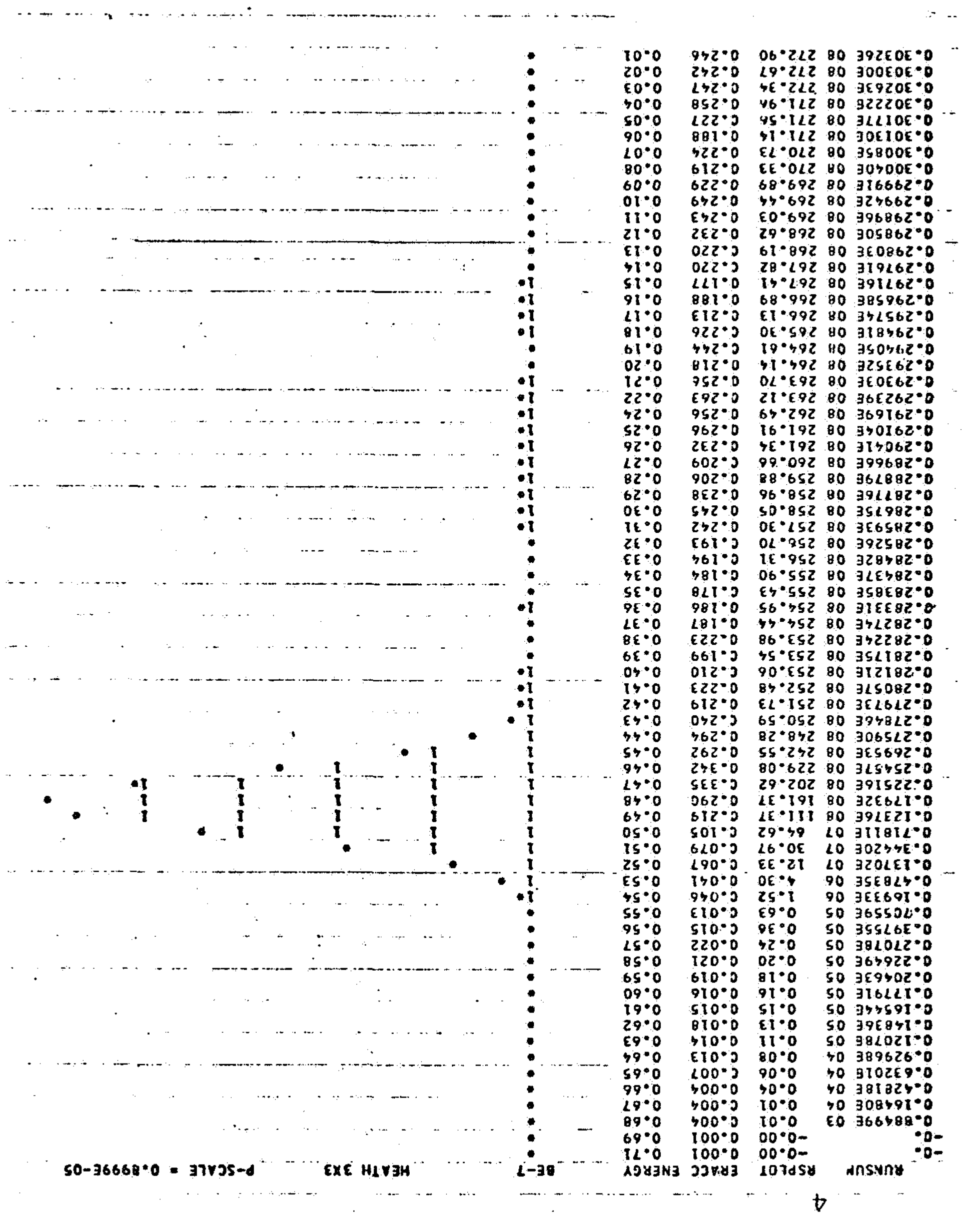

Fig. III-4. Unfolded Gamma Spectrum for ^{7}Be.

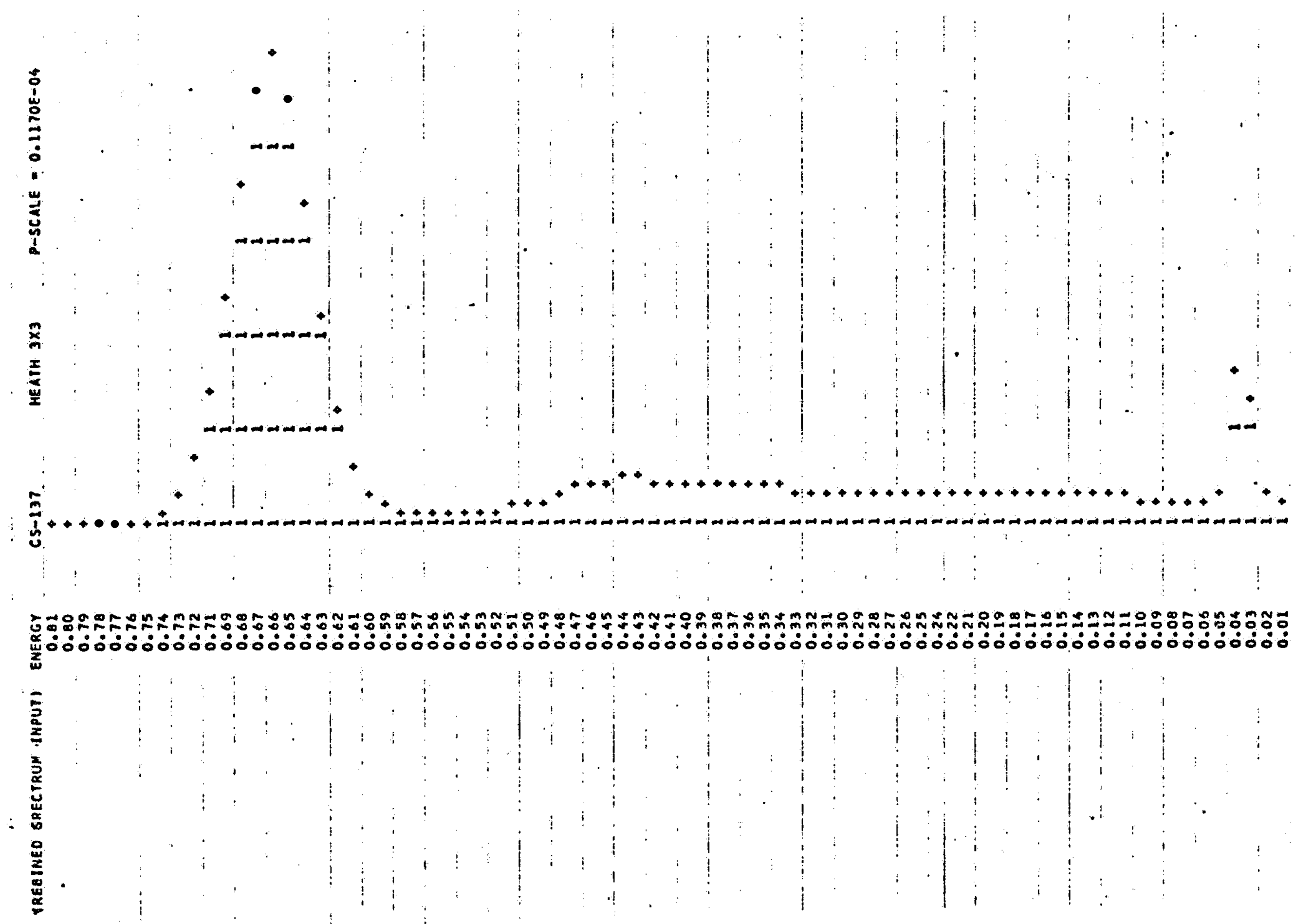

Fig. III-5. Corrected Pulse-Height Distribution for ^{137}Cs.

RUNSUM	RSPLOT	ERADC	ENERGY
0.83615E 02	0.00	C.001	0.81
0.37142E 04	0.04	0.007	0.80
0.96213E 04	0.11	C.009	0.79
0.12599E 05	0.15	C.010	0.78
0.20629E 05	0.24	C.018	0.77
0.39304E 05	0.46	0.025	0.76
0.78506E 05	0.92	0.07C	0.75
0.18111E 06	2.12	C.104	0.74
0.42632E 06	4.99	0.103	0.73
0.99745E 06	11.67	C.143	0.72
0.21674E 07	25.36	0.187	0.71
0.42407E 07	49.63	C.227	0.69
0.73507E 07	86.C3	C.401	0.68
0.11323E 08	132.51	0.444	0.67
0.15595E 08	182.51	0.457	0.66
0.19405E 08	227.10	C.630	0.65
0.22307E 08	261.06	0.857	0.64
0.24181E 08	282.99	0.881	0.63
0.25202E 08	294.94	0.994	0.62
0.25714E 08	300.93	C.897	0.61
0.25959E 08	303.80	C.938	0.60
0.26075E 08	305.16	C.963	0.59
0.26137E 08	305.88	0.978	0.58
0.26172E 08	306.29	C.947	0.57
0.26201E 08	306.63	C.894	0.56
0.26222E 08	306.87	0.896	0.55
0.26244E 08	307.13	0.876	0.54
0.26270E 08	307.44	C.909	0.53
0.26302E 08	307.81	0.907	0.52
0.26340E 08	308.25	C.915	0.51
0.26375E 08	308.67	0.918	0.50
0.26411E 08	309.09	C.941	0.49
0.26458E 08	309.64	C.954	0.48
0.26522E 08	310.38	C.962	0.47
0.26614E 08	311.46	0.876	0.46
0.26703E 08	312.51	C.765	0.45
0.26800E 08	313.65	C.684	0.44
0.26904E 08	314.85	0.719	0.43
0.26995E 08	315.92	0.764	0.42
0.27087E 08	317.00	C.790	0.41
0.27180E 08	318.08	C.781	0.40
0.27273E 08	319.18	0.816	0.39
0.27370E 08	320.31	0.853	0.38
0.27462E 08	321.38	C.820	0.37
0.27554E 08	322.47	0.848	0.36
0.27644E 08	323.52	0.787	0.35
0.27734E 08	324.57	0.829	0.34
0.27819E 08	325.56	C.870	0.33
0.27908E 08	326.61	C.886	0.32
0.27996E 08	327.64	C.941	0.31
0.28085E 08	328.68	0.962	0.30
0.28173E 08	329.71	C.992	0.29
0.28260E 08	330.73	1.003	0.28
0.28350E 08	331.78	1.000	0.27
0.28438E 08	332.81	1.023	0.26
0.28523E 08	333.81	1.097	0.25
0.28600E 08	334.70	1.043	0.24
0.28657E 08	335.37	1.046	0.22
0.28719E 08	336.10	1.032	0.21
0.28792E 08	336.95	C.951	0.20
0.28874E 08	337.92	C.974	0.19
0.28960E 08	338.92	0.937	0.18
0.29034E 08	339.78	C.903	0.17
0.29086E 08	340.39	C.920	0.16
0.29124E 08	340.83	C.905	0.15
0.29177E 08	341.45	0.950	0.14
0.29223E 08	342.00	C.946	0.13
0.29265E 08	342.49	C.957	0.12
0.29309E 08	343.00	0.966	0.11
0.29350E 08	343.48	0.969	0.10
0.29386E 08	343.91	C.943	0.09
0.29428E 08	344.39	C.927	0.08
0.29472E 08	344.91	C.930	0.07
0.29516E 08	345.42	0.884	0.06
0.29608E 08	346.50	C.933	0.05
0.30835E 08	360.86	1.031	0.04
0.31776E 08	371.87	1.C00	0.03
0.31887E 08	373.17	0.991	0.02
0.31923E 08	373.59	C.993	0.01

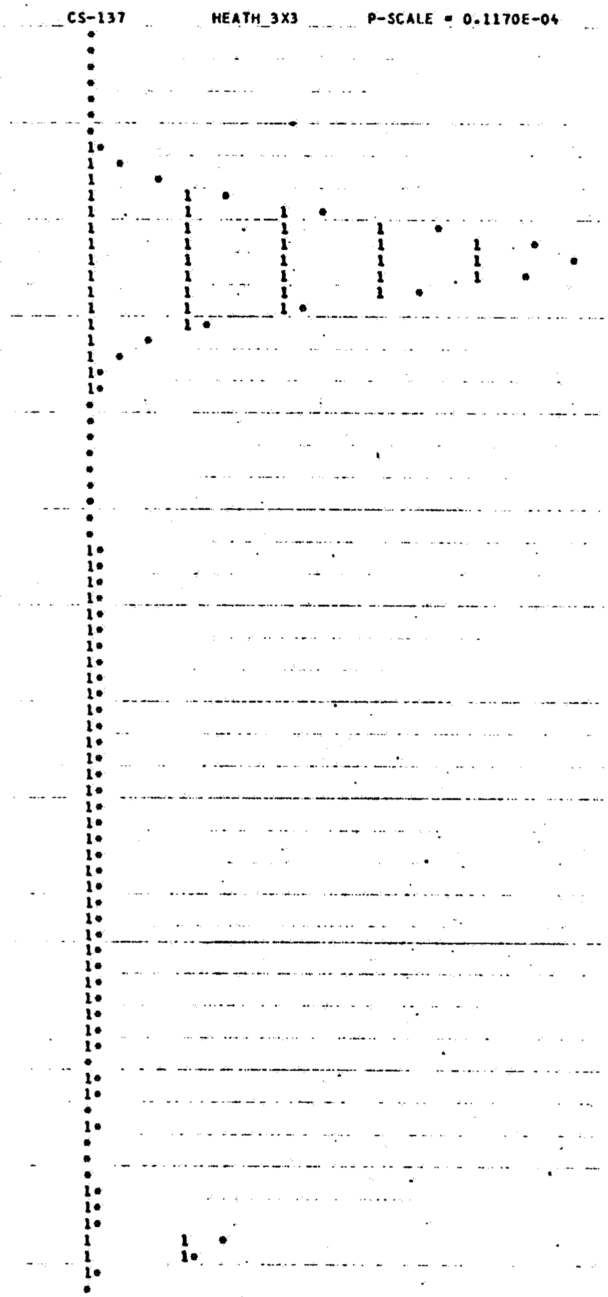

Fig. III-6. Unfolded Gamma Spectrum for ^{137}Cs.

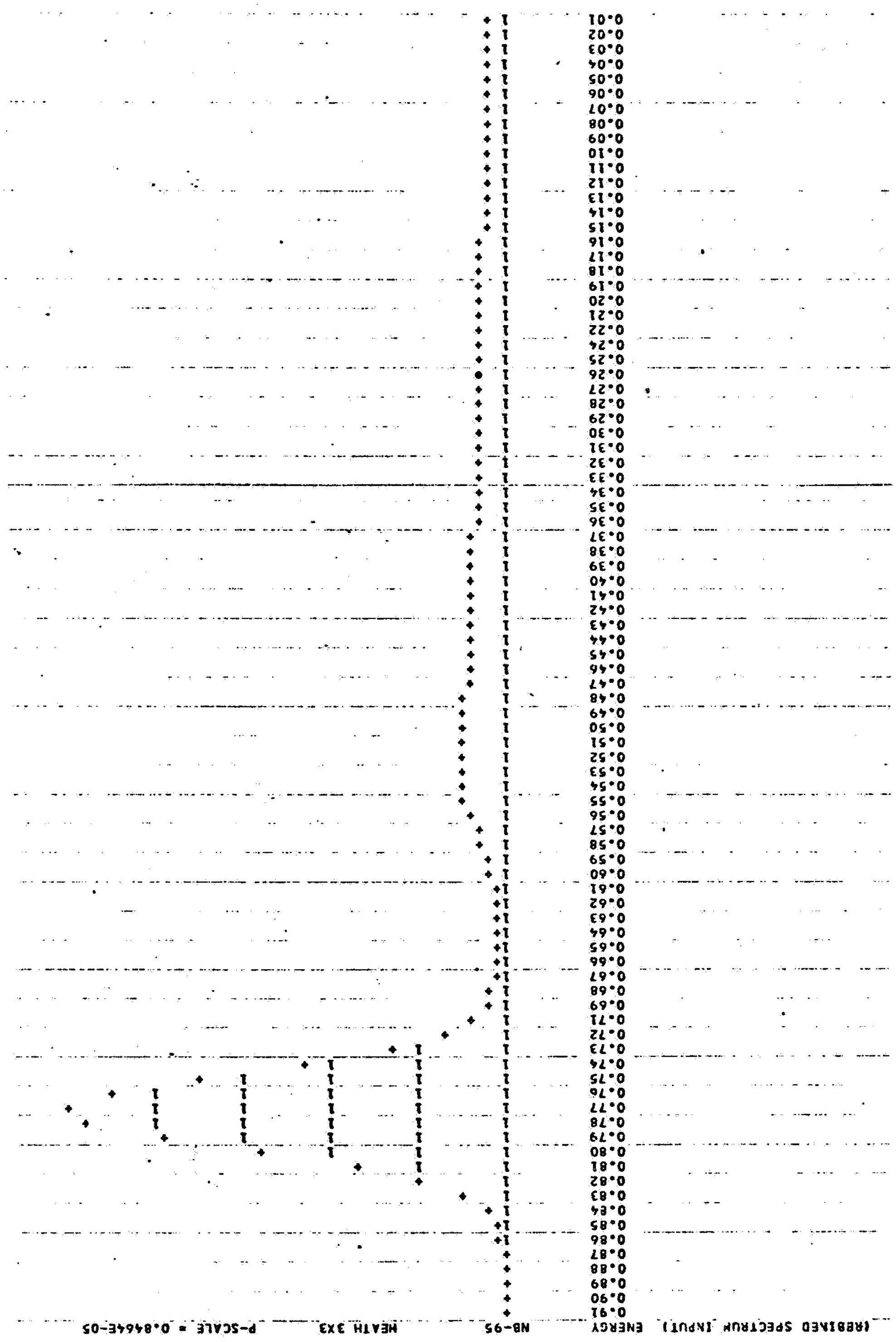

Fig. III-7. Corrected Pulse-Height Distribution for ^{95}Nb.

RUNSUM	RSPLOT	ERACC	ENERGY
0.94240E 03	0.01	0.002	0.91
0.61861E 04	0.05	0.005	0.90
0.14688E 05	0.12	0.006	0.89
0.31427E 05	0.27	0.007	0.88
0.60419E 05	0.51	0.016	0.87
0.12039E 06	1.02	0.021	0.86
0.24543E 06	2.08	0.010	0.85
0.51649E 06	4.37	0.032	0.84
0.10891E 07	9.22	0.128	0.83
0.22265E 07	18.85	0.073	0.82
0.42901E 07	36.31	0.165	0.81
0.76112E 07	64.42	0.270	0.80
0.12248E 08	103.67	0.219	0.79
0.17920E 08	151.67	0.226	0.78
0.23827E 08	201.67	0.322	0.77
0.29132E 08	246.57	0.353	0.76
0.33246E 08	281.40	0.690	0.75
0.36007E 08	304.76	0.817	0.74
0.37590E 08	318.16	0.816	0.73
0.38454E 08	325.47	0.852	0.72
0.38873E 08	329.02	0.818	0.71
0.39088E 08	330.84	0.806	0.69
0.39206E 08	331.84	0.780	0.68
0.39268E 08	332.37	0.809	0.67
0.39302E 08	332.65	0.822	0.66
0.39325E 08	332.84	0.831	0.65
0.39343E 08	333.00	0.876	0.64
0.39367E 08	333.20	0.863	0.63
0.39396E 08	333.45	0.888	0.62
0.39431E 08	333.74	0.900	0.61
0.39472E 08	334.09	0.860	0.60
0.39519E 08	334.49	0.888	0.59
0.39580E 08	335.01	0.949	0.58
0.39650E 08	335.60	0.956	0.57
0.39748E 08	336.42	0.908	0.56
0.39884E 08	337.57	0.873	0.55
0.40028E 08	338.80	0.928	0.54
0.40173E 08	340.02	0.866	0.53
0.40318E 08	341.25	0.858	0.52
0.40453E 08	342.39	0.886	0.51
0.40586E 08	343.52	0.875	0.50
0.40715E 08	344.61	0.908	0.49
0.40860E 08	345.84	0.912	0.48
0.41005E 08	347.07	0.906	0.47
0.41156E 08	348.34	0.928	0.46
0.41308E 08	349.63	0.893	0.45
0.41444E 08	350.78	0.839	0.44
0.41583E 08	351.96	0.802	0.43
0.41717E 08	353.09	0.808	0.42
0.41857E 08	354.28	0.812	0.41
0.41989E 08	355.40	0.781	0.40
0.42103E 08	356.36	0.755	0.39
0.42222E 08	357.37	0.794	0.38
0.42336E 08	358.34	0.723	0.37
0.42441E 08	359.22	0.715	0.36
0.42545E 08	360.10	0.696	0.35
0.42644E 08	360.94	0.700	0.34
0.42758E 08	361.90	0.711	0.33
0.42853E 08	362.71	0.706	0.32
0.42955E 08	363.57	0.756	0.31
0.43048E 08	364.35	0.756	0.30
0.43140E 08	365.13	0.746	0.29
0.43235E 08	365.94	0.694	0.28
0.43326E 08	366.71	0.693	0.27
0.43410E 08	367.42	0.702	0.26
0.43493E 08	368.13	0.764	0.25
0.43544E 08	368.56	0.721	0.24
0.43600E 08	369.03	0.724	0.22
0.43675E 08	369.66	0.714	0.21
0.43768E 08	370.45	0.705	0.20
0.43862E 08	371.25	0.730	0.19
0.43933E 08	371.85	0.710	0.18
0.43977E 08	372.22	0.695	0.17
0.44006E 08	372.47	0.670	0.16
0.44046E 08	372.81	0.633	0.15
0.44086E 08	373.15	0.653	0.14
0.44122E 08	373.44	0.656	0.13
0.44151E 08	373.70	0.660	0.12
0.44181E 08	373.95	0.668	0.11
0.44209E 08	374.18	0.671	0.10
0.44236E 08	374.41	0.650	0.09
0.44267E 08	374.67	0.638	0.08
0.44296E 08	374.92	0.642	0.07
0.44322E 08	375.14	0.605	0.06
0.44349E 08	375.37	0.640	0.05
0.44378E 08	375.62	0.668	0.04
0.44419E 08	375.97	0.656	0.03
0.44453E 08	376.25	0.649	0.02
0.44484E 08	376.52	0.651	0.01

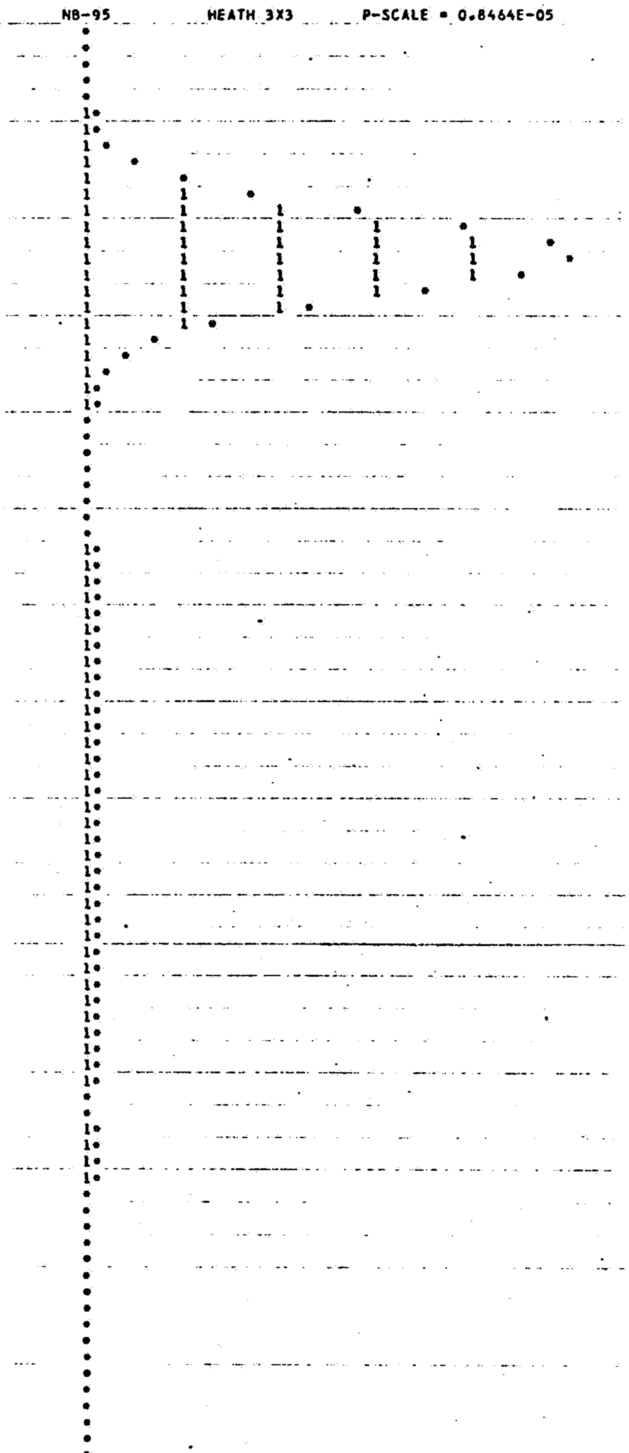

Fig. III-8. Unfolded Gamma Spectrum for ^{95}Nb.

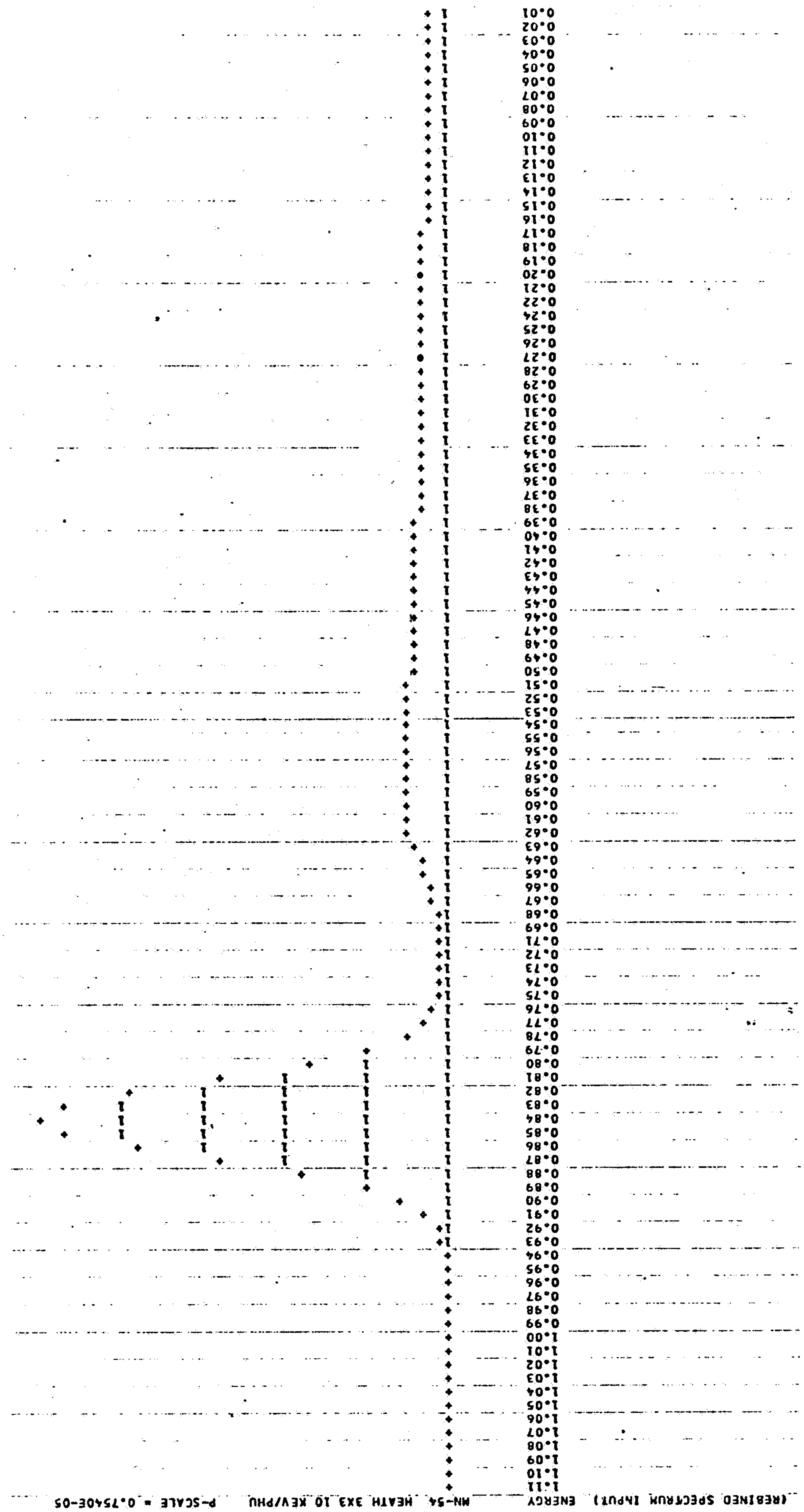

Fig. III-9. Corrected Pulse-Height Distribution for ^{54}Mn.

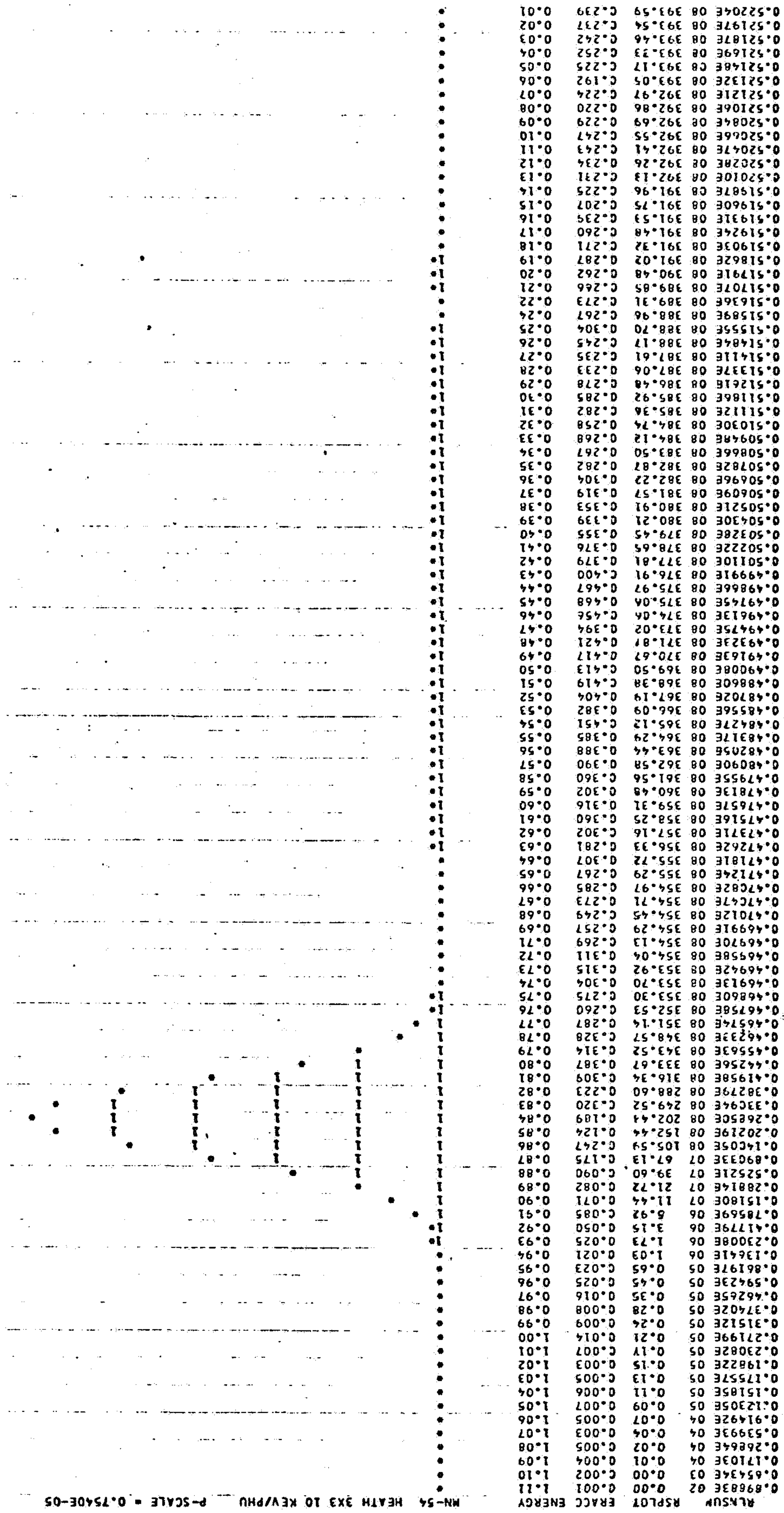

Fig. III-10. Unfolded Gamma Spectrum for ^{54}Mn.

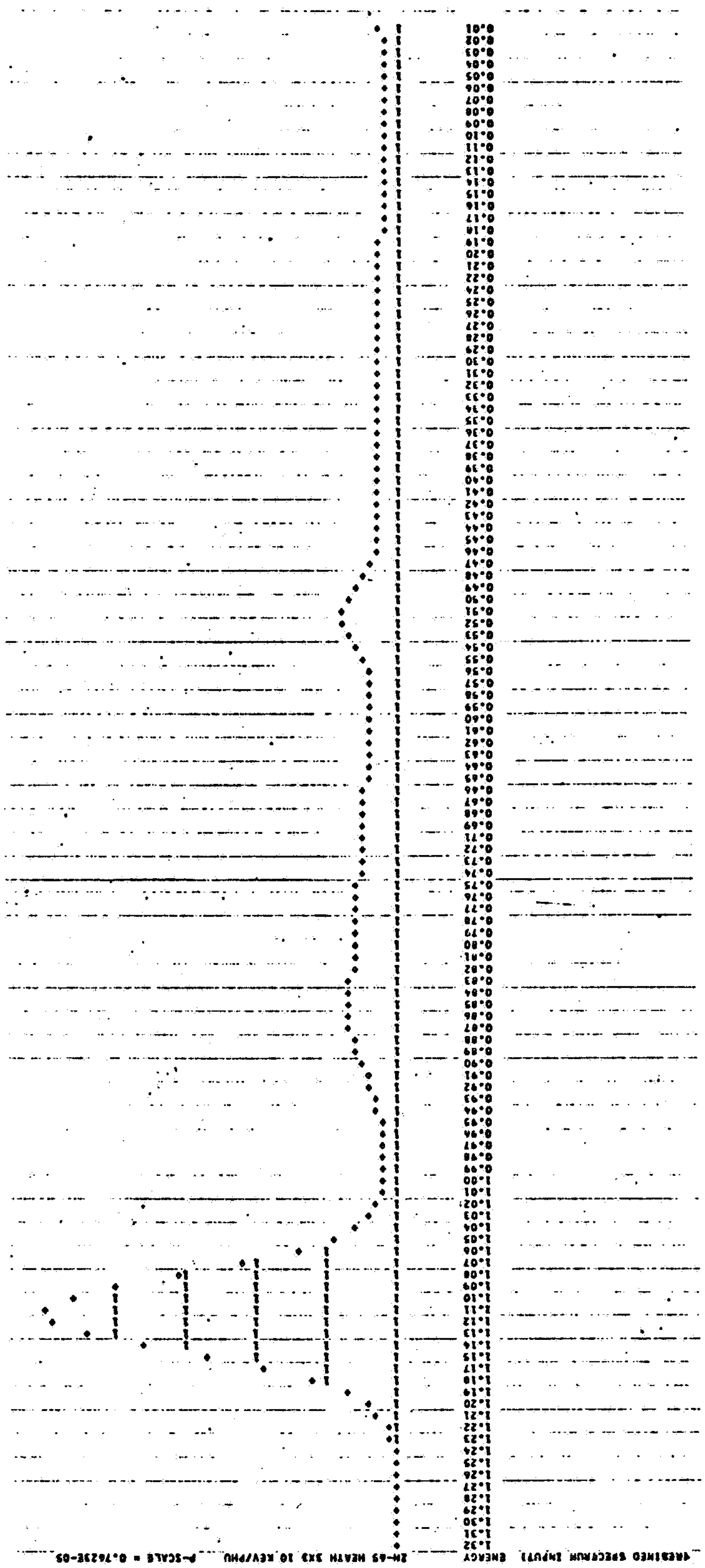

Fig. III-11. Corrected Pulse-Height Distribution for ^{65}Zn.

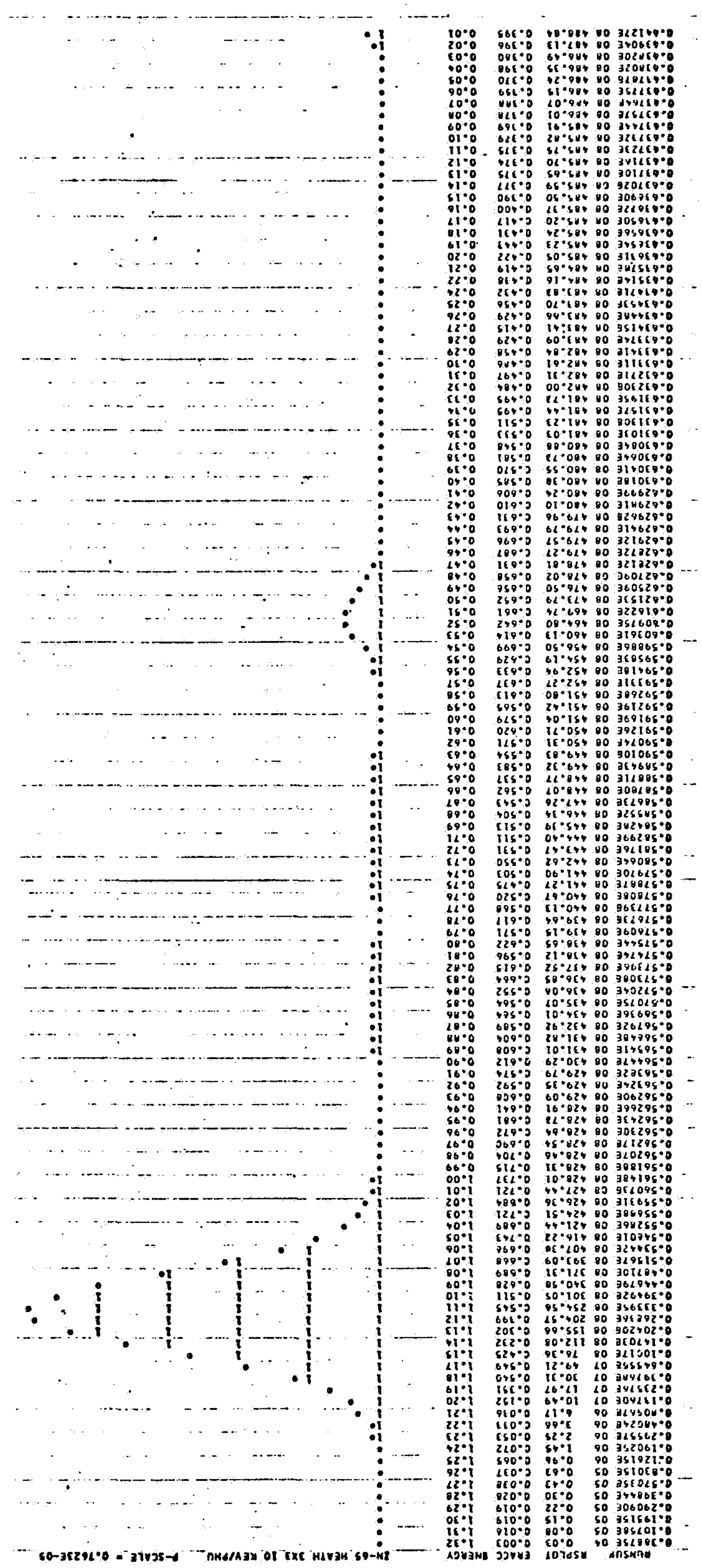

Fig. III-12. Unfolded Gamma Spectrum for ^{65}Zn.

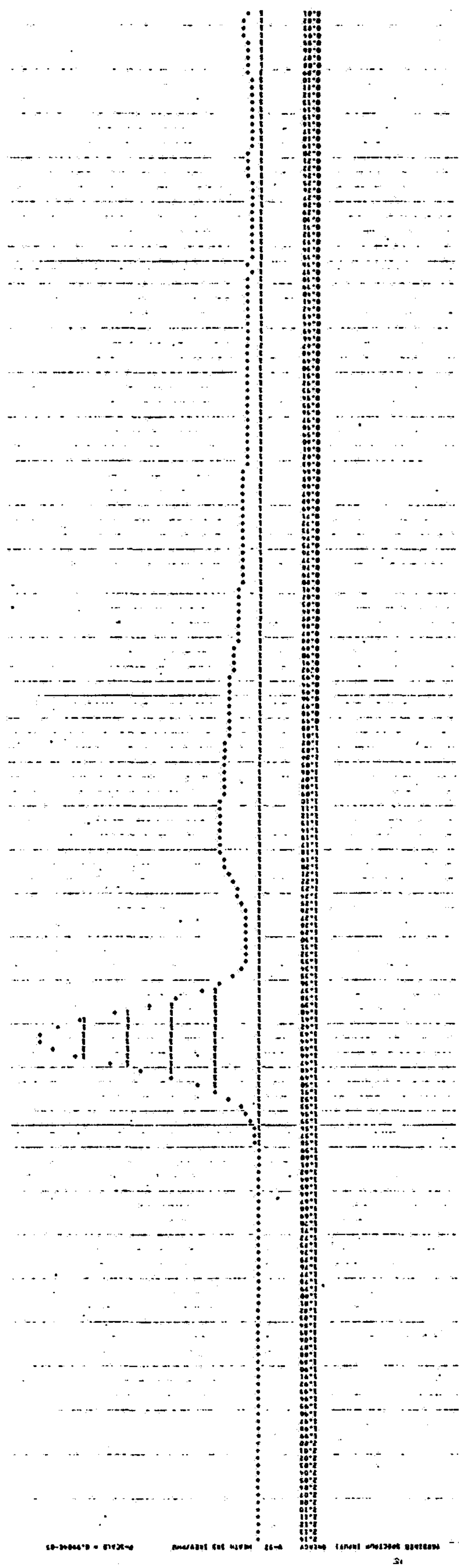

Fig. III-13. Corrected Pulse-Height Distribution for ^{52}V.

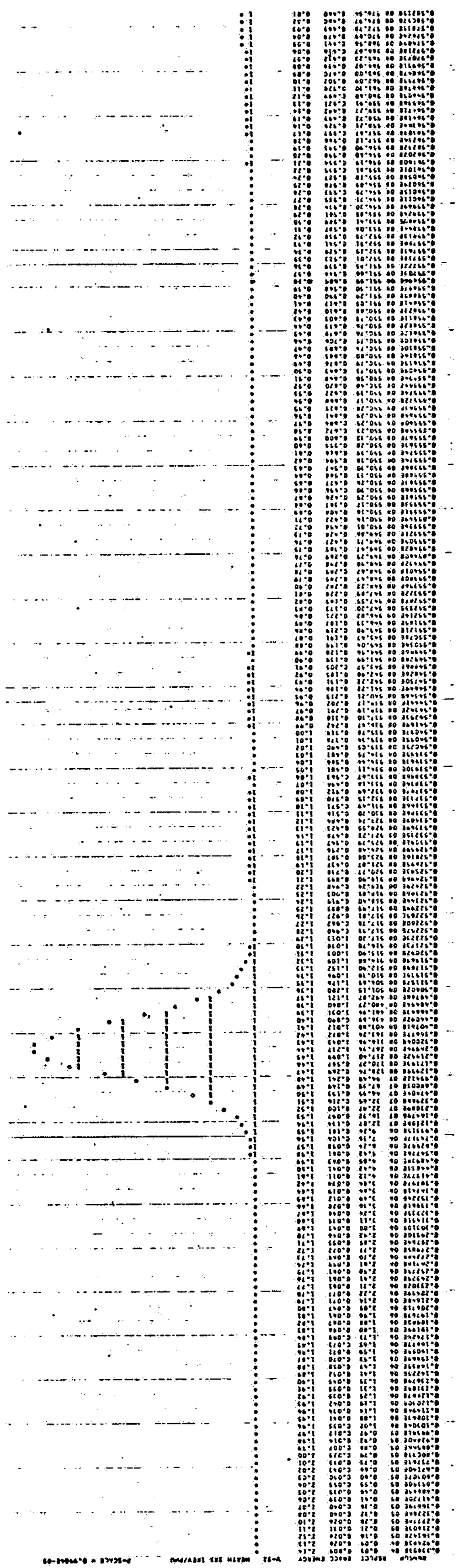

Fig. III-14. Unfolded Gamma Spectrum for ^{52}V.

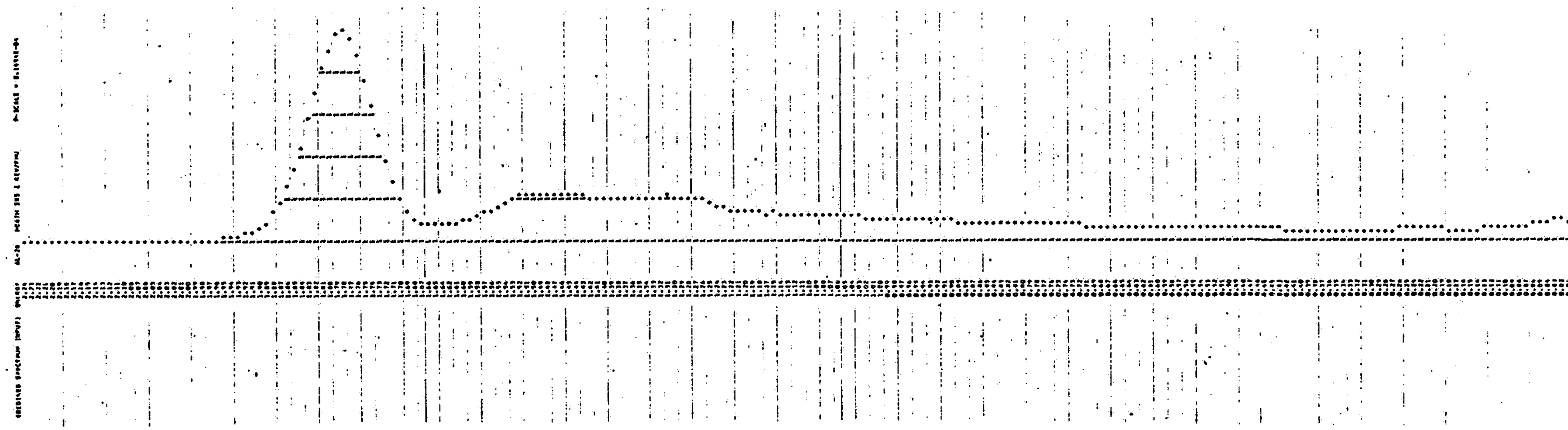

Fig. III-15. Corrected Pulse-Height Distribution for ^{28}Al.

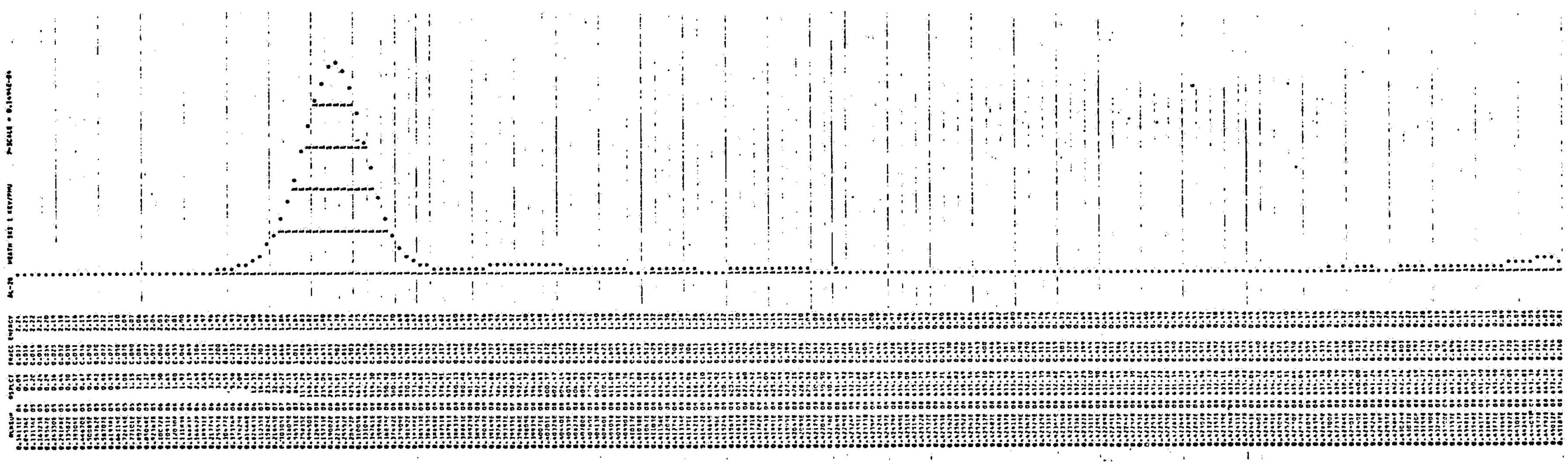

Fig. III-16. Unfolded Gamma Spectrum for ^{28}Al.

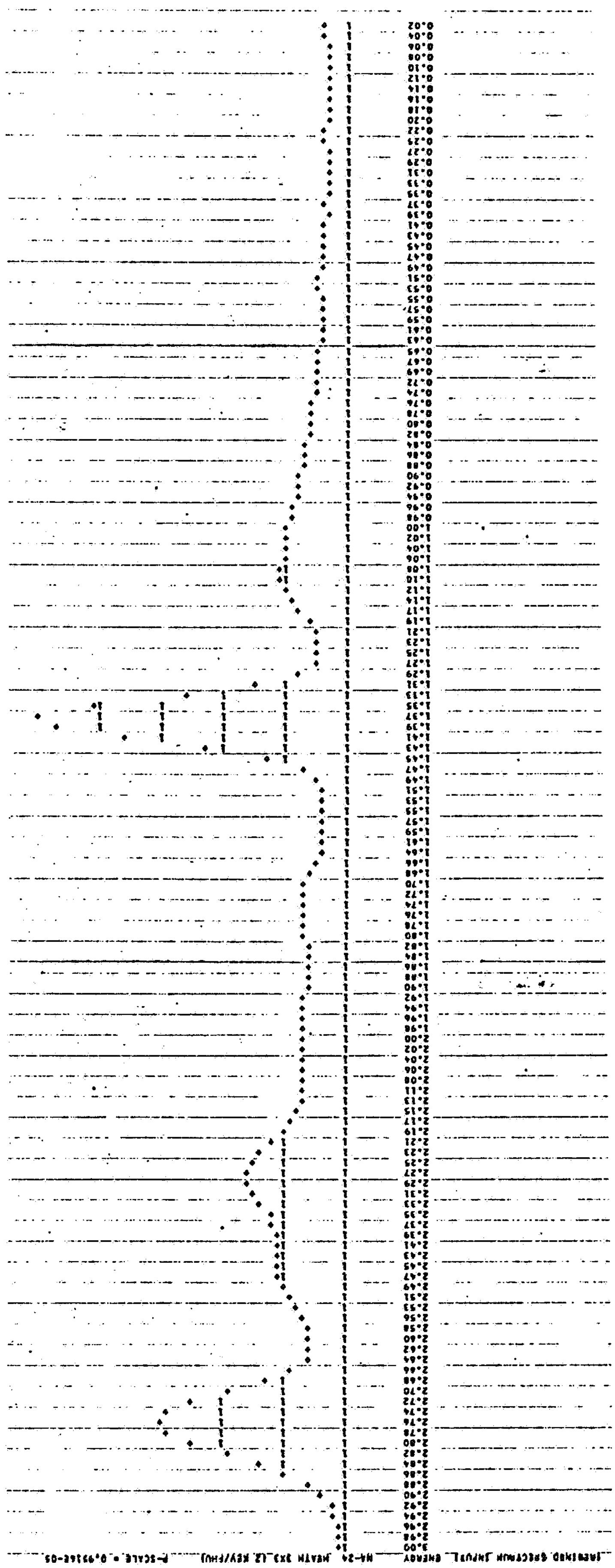

Fig. III-17. Corrected Pulse-Height Distribution for ^{24}Na.

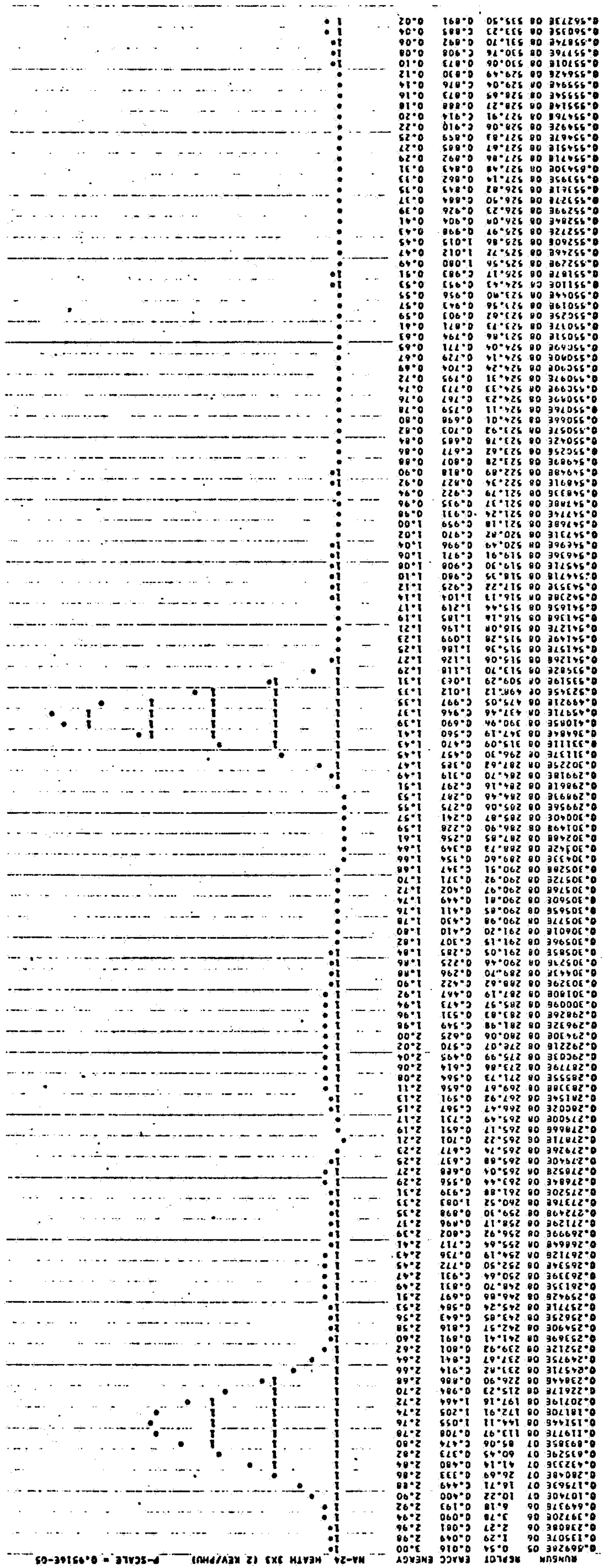

Fig. III-18. Unfolded Gamma Spectrum for ^{24}Na.

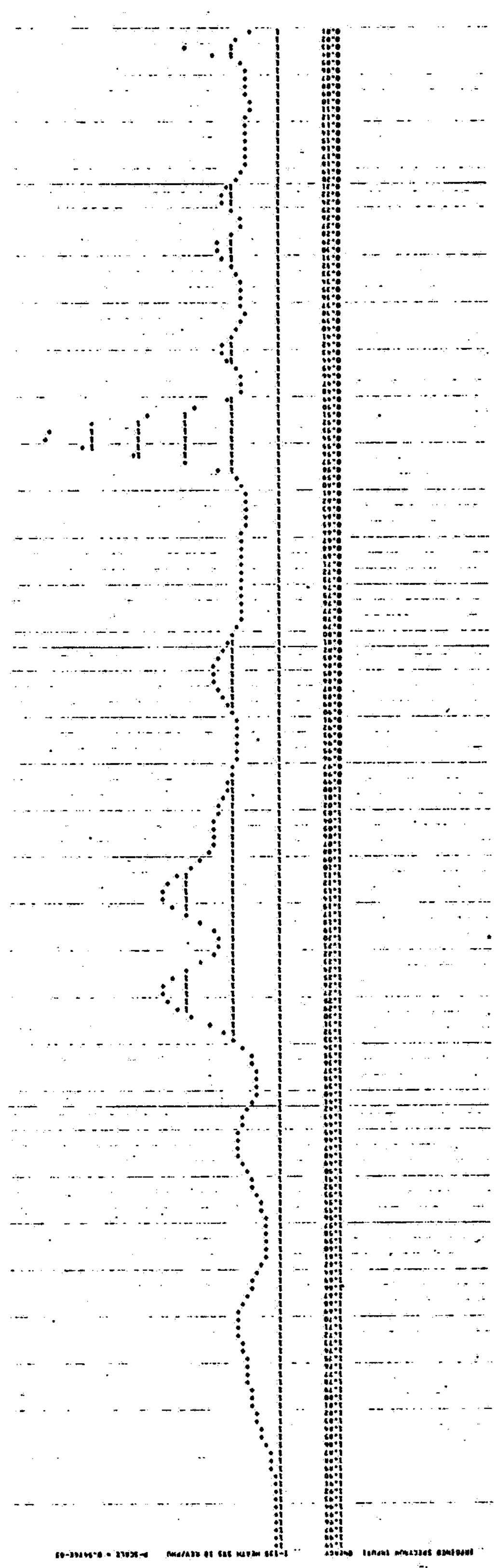

Fig. III-19. Corrected Pulse-Height Distribution for ^{135}I.

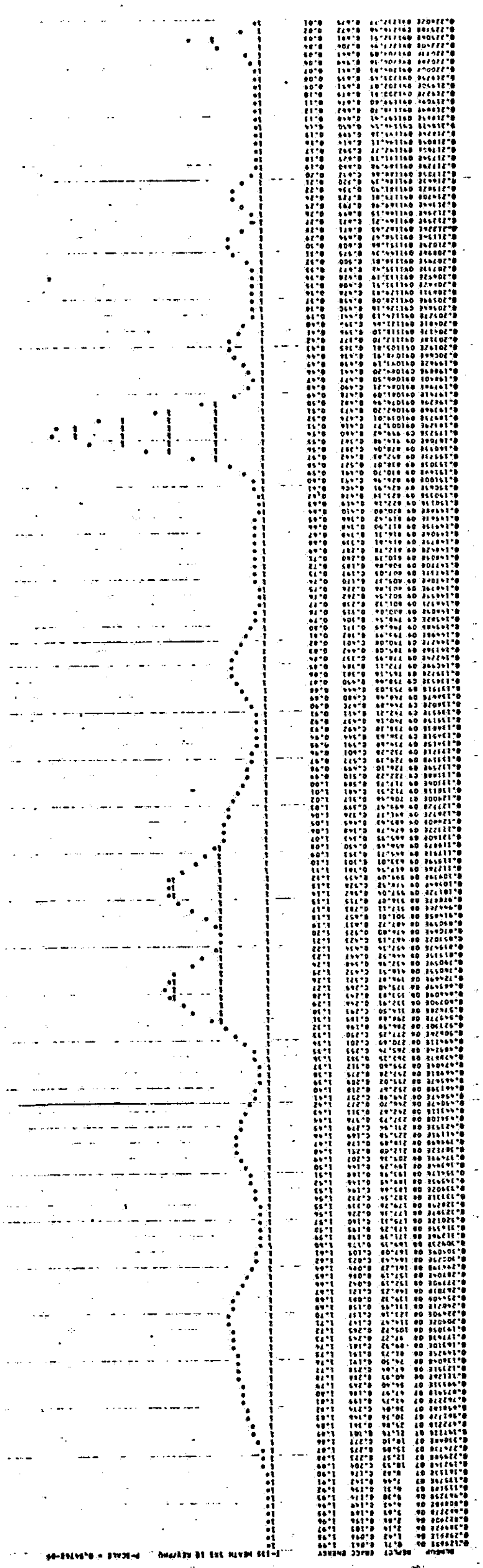

Fig. III-20. Unfolded Gamma Spectrum for ^{135}I.

NASA LISTING

Tino Ahrens, Advanced Research Corporation, 715 Miami Circle, N. E., Atlanta, Georgia 30324

Louis Avrami, Explosives Laboratory, Bldg. 407, Pictinny Arsenal, Dover, New Jersey 07301

M. Awschalom, Princeton Penn. Accelerator, P. O. Box 682, Princeton, New Jersey 08540

M. Barbier, CERN, Geneva, Switzerland

N. Barr, Radiological Physics Branch, Division of Biology and Medicine, U. S. Atomic Energy Commission, Washington, D. C. 20545 (5 copies)

C. K. Bauer, Dept. 72-34, Lockheed-Georgia Company, Marietta, Georgia 30060

P. R. Bell, TH, Chief of Lunar and Earth Sciences Division, Manned Spacecraft Center-NASA, Houston, Texas 77058

S. Bresticker, Grumman Aircraft Engineering Corp., Space Sciences Group, Plant 5, Bethpage, L. I., New York 11714

Brooks Air Force Base, Radiobiology Department, Chief, San Antonio, Texas 78235

M. O. Burrell, M-RP-NIP, National Aeronautics and Space Adm., Marshall Space Flight Center, Huntsville, Alabama 35812

B. W. Colston, U. S. Atomic Energy Commission, Sandia Area Office, P. O. Box 5400, Albuquerque, New Mexico 87115

R. G. Cochran, Department of Nuclear Engineering, A and M College of Texas, College Station, Texas

Ted Colvin, Bendix Systems Division, 3300 Plymouth Road, Ann Arbor, Michigan 48105

Director, Defense Atomic Support Agency, Pentagon, Washington, D. C. 20301

Charles A. Dempsey, 6570 AMRL (MRT), Wright-Patterson AFB, Ohio 45433

Herman J. Donnert, U. S. Army Nuclear Defense Laboratory, AMXND-C, Edgewood Arsenal, Maryland 21010

D. W. Drawbaugh, Westinghouse Electric Corp., Astronuclear Laboratory, P. O. Box 10864, Pittsburgh, Pennsylvania 15236

John E. Duberg, National Aeronautics and Space Adm., Langley Research Center, Langley Field, Virginia 23365

D. L. Dyd, The Boeing Company, Mail Stop S3-72, Seattle, Washington 98124

Nat Edmunson, Code R-RP-N, National Aeronautics and Space Adm., Marshall Space Flight Center, Huntsville, Alabama 35812

Robley D. Evans, Professor of Physics, Room 6-315, Massachusetts Institute of Technology, Cambridge, Massachusetts 02139

E. M. Finkelman, Grumman Aircraft Engineering Corp., LEM Project, Plant 25, Bethpage, L. I., New York 11714

Trutz Foelsche, National Aeronautics and Space Adm., Langley Research Center, Langley Field, Virginia 23365

R. E. Fortney, Northrop Space Laboratories, 3401 West Broadway, Hawthorne, California 90250

Leo Fox, Code RBH, Biotechnology and Human Research Division, National Aeronautics and Space Adm., Washington, D. C. 20546

Stan Freden, Aerospace Corp., Box 95085, Los Angeles, California 90045

R. C. Good, Jr., General Electric Company, Room M7023H - VFSTC, P. O. Box 8555, Philadelphia, Pennsylvania 19101

F. Gordon, Code 716, National Aeronautics and Space Adm., Goddard Space Flight Center, Greenbelt, Maryland 10027

Raymond M. Hansen, MS 235, National Aeronautics and Space Adm., Langley Research Center, Mail Stop 235, Langley Field, Virginia 23365

Harry Harrison, Code RRE, National Aeronautics and Space Adm., Hdqts., Washington, D. C. 20546

Russell Heath, Phillips Petroleum Company, P. O. Box 2067, Idaho Falls, Idaho 83401

Herbert D. Hendricks, National Aeronautics and Space Adm., Langley Research Center, MS499, Langley Field, Virginia 23365

W. N. Hess, National Aeronautics and Space Adm., Goddard Space Flight Center, Greenbelt, Maryland 20771

R. H. Hilberg, Bellcomm, Inc., 1100 17th Street, N.W., Washington, D. C. 20036

Charles W. Hill, Dept. 73-69, Zone 280, Lockheed-Georgia Company, Marietta, Georgia 30060

J. T. Holloway, Grants and Research Contracts, Office of Space Sciences, National Aeronautics and Space Adm., Washington, D. C. 20546 (5 copies)

William C. Hulten, National Aeronautics and Space Adm., Mail Stop 235, Langley Research Center, Langley Field, Virginia 23365

Lt. Joseph F. Janni, WLRB-1, Air Force Weapons Laboratory, Kirtland Air Force Base, New Mexico 87117

Dale W. Jenkins, Chief, Environmental Biology, Office of Space Sciences, NASA, Washington, D. C. 20546

Philippe Tardy-Joubert, Serv De Protection Contre Les Radiation, Centre D Etudes Nucleaires De Saclay, B. P. No. 2, Gif-Sur-Yvette (Seine et Oise), FRANCE

Clyde Jupiter, General Atomic, P. O. Box 608, San Diego, California 92112

Irving Karp, NASA/Lewis Research Center, Cleveland, Ohio 44135

Ludwig Katz, Air Force Cambridge Research Center, L. G. Hanscom Field, Massachusetts

Glenn Keister, Boeing Airplane Company, Aerospace Division, P. O. Box 3707, Seattle, Washington 98124

J. Warren Keller, Code RV-1, National Aeronautics and Space Adm., Washington, D. C. 20546 (3 copies)

James F. Kenny, Boeing Scientific Research Laboratory, P. O. Box 3981, Seattle, Washington 98124

E. C. Kidd, Zone S71, Dept. 61-2, General Dynamics/Fort Worth, P. O. Box 748, Fort Worth, Texas 76101

Robert L. Kloster, McDonnell Aircraft Corp., P. O. Box 516, St. Louis, Missouri 63166

George A. Kilstad, Assistant Director Physics-Math Programs, Division of Research, U. S. Atomic Energy Commission, Washington, D. C. 20545

Eugene B. Konecci, Department of Management BEOB-200, University of Texas, Austin, Texas 78712

W. Kreger, Code 940, U. S. Naval Radiological Defense Laboratory, San Francisco, California 94135

Ed Kuhn, Republic Aviation Corporation, Power Conversion Systems Division, Farmingdale, L. I., New York 11735

Wright H. Langham, Los Alamos Scientific Laboratory, Los Alamos, New Mexico 87544

Borje Larsson, University of Uppsala, The Gustaf Werner Institute, Uppsala, Sweden

J. M. Lavie, Centre D. Etudes Nucleaires, De Saclay, S.E.C.R.-B. P. No. 2, 91 Gif-Sur-Yvette, France

Martin Leimdorfer, Industri-Matematik AB, De Geersgatan 8, Stockholm No. Sweden

S. H. Levine, Northrop Space Laboratories, 3401 W. Broadway, 2452/61 Hawthorne, California 90250

Lynn R. Lewis, Dept. 250, Bendix Systems Division, 3300 Plymouth Road, Ann Arbor, Michigan 48105

John R. Lilley, A-830-BBFO-78, Missile Space Systems Division, Douglas Aircraft Co., Inc., Santa Monica, California

Major Russell E. Linkous, Air Force Systems Command (SCTR), Andrews AFB, Maryland 20331

Robert Macklin, Jet Propulsion Laboratory, Pasadena, California 91103

Brian Mar, Boeing Airplane Co., MS 23-82, Aerospace Division, P. O. Box 3707, Seattle, Washington 98124

J. Scanlon, Research Department, Grumman Aircraft Engineering Corp., Bethpage, New York 11714

Thomas J. McGuire, Systems Engineering Group (SESSV), Wright-Patterson AFB, Ohio 45433

E. J. McLaughlin, Space Medicine, NASA - Code MM, Washington, D. C. 20546

R. V. Meghreblian, Jet Propulsion Laboratory, 4800 Oak Grove Drive, Pasadena, California 91103

Albert E. Metzger, Jet Propulsion Laboratory, 354-401F, 4800 Oak Grove, Pasadena, California

J. M. Miller, Chemistry Department, Columbia University, New York, New York 10027

R. A. Miller, Zone S71, Dept. 61-2, General Dynamics/Forth Worth, P. O. Box 748, Fort Worth, Texas 76101

Jerry L. Modisette, National Aeronautics and Space Adm., Manned Spacecraft Center, Houston, Texas 77001 (5 copies)

Winnie M. Morgan, Technical Reports, Grants and Research Contracts, Office of Space Sciences, NASA, Washington, D. C. 20546 (25 copies)

Capt. J. D. Munson, Space Systems Division (SSTDS), Los Angeles Air Force Station, Los Angeles, California 90045

Sam V. Nablo, Ion Physics Corporation, Burlington, Massachusetts 01803

R. R. Nash, Code RRM, National Aeronautics and Space Adm., Washington, D. C. 20546

John P. Neissel, MC-506, 175 Courtner Avenue, General Electric Company, San Jose, California 95125

Maynard Pearson, Boeing Airplane Company, Aerospace Division, P. O. Box 3707, Seattle, Washington 98124

Col. John E. Pickering, USAF, National Aeronautics and Space Adm. (Code MM), Washington, D. C. 20546

G. F. Pieper, Code 600, National Aeronautics and Space Adm., Goddard Space Flight Center, Greenbelt, Maryland 10027

Robert Pruett, P. O. Box 95085, Los Angeles, California 90045

Arthur Reetz, Code RV-1, National Aeronautics and Space Adm., Washington, D. C. 20546 (3 copies)

O. Reynolds, Director, Bio-Science Programs, Office of Space Sciences, National Aeronautics and Space Adm., Washington D. C. 20546 (5 copies)

Roberg G. Riedesel, Douglas Aircraft Company, Missile and Space Division, 3000 Ocean Park Blvd., Santa Monica, California 90405

Don Robbins, ET32, National Aeronautics and Space Adm., Manned Spacecraft Center, Houston, Texas 77058

H. J. Schaefer, U. S. Naval School of Aviation Medicine, U. S. Naval Aviation Medical Center-54, Pensacola, Florida 32512

W. Wayne Scott, Chattanooga State Technical Institute, 4501 Amnico Highway, Chattanooga, Tennessee 37401

Robert L. Seale, University of Arizona, Tucson, Arizona 85721

Jerome L. Shapiro, Division Engineering and Applied Science, Pasadena, California 91109

R. D. Shelton, Code R-RP-N, National Aeronautics and Space Adm., Marshall Space Flight Center, Huntsville, Alabama

Robert T. Siegel, Department of Physics, College of William and Mary, Williamsburg, Virginia 23185

J. J. Singh, M.S. 234, NASA, Langley Research Center, Langley Station, Hampton, Virginia 23365

G. D. Smith, Ames Research Center, Moffett Field, California 94035

Jerry Speakman, 6570 AMRL (MRBBR), Wright-Patterson AFB, Ohio

Dwain F. Spencer, Jet Propulsion Laboratory, Pasadena, California 31103

William Steigelmann, Kuljian Corp., 1200 North Broad Street, Philadelphia, Pennsylvania 19121

Henry Stern, R-RP-N, NASA, Marshall Space Flight Center, Huntsville, Alabama 35812

T. R. Strayhorn, S-71, General Dynamics, Fort Worth, Texas 76101

S. Tom Taketa, Mail Stop N 236-5, NASA, Ames Research Center, Mofett Field, California 94035

Cornelius Tobias, University of California, Lawrence Radiation Laboratory, Berkeley, California 94720

Jacob I. Trombka, Code SM, National Aeronautics and Space Adm., Washington, D. C. 20546

Werner Von Braun, Director, George C. Marshall Space Flight Center, NASA, Huntsville, Alabama 35812

G. P. Wachtell, Franklin Institute, 20th and Parkway, Philadelphia, Pennsylvania 19103

Roger Wallace, University of California, Bldg. 72, Lawrence Radiation Laboratory, Berkeley, California 94720

G. T. Western, Y-71, General Dynamics, Fort Worth, Texas 76101

Glenn A. Whan, Associate Professor, Nuclear Engineering Laboratory, The University of New Mexico, Albuquerque, New Mexico 87106

Ralph Wiley, Mail Zone Y-42, P. O. Box 748, Fort Worth, Texas 76101

Maurice Wilkinson, The Boeing Company, M.S. 23-82, Seattle, Washington 98124

W. R. Yucker, A-2-833, Douglas Aircraft Co., Nuclear Department, 3000 Ocean Park Boulevard, Santa Monica, California 90405

Marcello Zocchi, Reactor and Radiation, National Bureau of Standards, Washington, D. C. 20234

K. Ziock, Department of Physics, University of Virginia, Charlottesville, Virginia 32901

Donald W. Aitken, Research Physicist, Stanford University, Department of Physics, Stanford, California

Wayne A. Coleman, Box 856, Edgewood, Maryland 21040

S. B. Curits, Building 29, Room 213, Lawrence Radiation Laboratory, Berkeley, California 94720

Sherwin M. Beck, M. S. 400, National Aeronautics and Space Administration, Langley Research Center, Hampton, Virginia

Elie Gradsztajan, Institut de Physique Nucleaire, B. P. 1, 91-Orsay, France

Charles Sondhaus, University of California College of Medicine, 1721 Giffin Avenue, Los Angeles, California 90031

William R. Mills, Field Research Laboratory, Socony Mobile Oil Co., Inc. P. O. Box 900, Dallas, Texas 75221

TM-2172

INTERNAL DISTRIBUTION

1-3. L. S. Abbott
4. V. R. Cain
5. C. E. Clifford
6. L. B. Holland
7. W. E. Kinney
8. T. A. Love
9-10. F. C. Maienschein
11. F. J. Muckenthaler
12. R. W. Peelle
13. S. K. Penny
14. F. G. Perey
15. R. T. Santoro
16. G. de Saussure
17. E. G. Silver
18. E. Straker
19. D. Sundberg
20. D. K. Trubey
21. J. W. Wachter
22. W. Zobel
23. E. R. Cohen (consultant)
24. B. C. Diven (consultant)
25. W. N. Hess (consultant)
26. M. H. Kalos (consultant)
27. L. V. Spencer (consultant)
28-29. Central Research Library
30. Document Reference Section
31-45. Laboratory Records Department
46. Laboratory Records ORNL RC
47. ORNL Patent Office

EXTERNAL DISTRIBUTION

48. P. B. Hemmig, Division of Reactor Development and Technology, U. S. Atomic Energy Commission, Washington, D. C.
49. I. F. Zartman, Division of Reactor Development and Technology, U. S. Atomic Energy Commission, Washington, D. C.
50. H. Goldstein, 242 Mudd Building, Columbia University, New York
51-65. Division of Technical Information Extension (DTIE)
66. Laboratory and University Division (ORO)
67-81. W. R. Burrus, Tennecomp, Inc., P. O. Box J, Oak Ridge, Tennessee
82-96. M. Young, Louisiana State University, Baton Rouge, Louisiana.
97-252. Given NASA Distribution as shown on preceding pages.